



**Chicken fat for catalysis: a scaffold is as important for molecular complexes for energy transformations as it is for enzymes in catalytic function**

Journal:	<i>Sustainable Energy &amp; Fuels</i>
Manuscript ID	SE-REV-04-2019-000229.R1
Article Type:	Review Article
Date Submitted by the Author:	29-Aug-2019
Complete List of Authors:	Laureanti, Joseph; Pacific Northwest National Lab O'Hagan, Molly; Montana State University Bozeman Shaw, Wendy; Pacific Northwest National Lab,

## **Chicken fat for catalysis: a scaffold is as important for molecular complexes for energy transformations as it is for enzymes in catalytic function**

Joseph A. Laureanti<sup>a</sup>, Molly O'Hagan<sup>b</sup>, and Wendy J. Shaw<sup>a</sup>

<sup>a</sup>Physical and Computational Sciences Directorate, Pacific Northwest National Laboratory, Richland, WA 99352, USA.

<sup>b</sup>Department of Chemistry and Biochemistry, Montana State University, Bozeman, MT 59717, USA.

### **Biographies**

**Joseph A. Laureanti.** Dr. Laureanti received his PhD in biochemistry in 2017 from Arizona State University. He currently works on design and analysis of artificial enzymes for energy relevant applications at Pacific Northwest National laboratory. His enzymatic design work focuses on tailoring small molecules for immobilization within protein environments to convert dihydrogen and store renewable energy as liquid fuels.



**Molly O'Hagan.** Dr. O'Hagan received her PhD in biochemistry from the University of Delaware in 2010 working on synthetic peptide models of metalloenzyme active sites. As a staff scientist at Pacific Northwest National Laboratory, her research was centered on designing molecular catalysts for energy related transformations. This work was focused on understanding how to control the structural dynamics of molecular nickel catalysts for hydrogen production to improve

catalytic performance, and the design of artificial metalloenzymes systems for catalytic CO<sub>2</sub> hydrogenation. Currently, she is a teaching professor in the Department of Chemistry and Biochemistry at Montana State University in beautiful Bozeman, MT.



**Wendy J. Shaw.** Dr. Shaw received her PhD in biophysical chemistry in 2000 from the University of Washington and has an emphasis in her research of understanding and mimicking nature. She currently works on biomineralization and energy related research at Pacific Northwest National laboratory. Her energy related work focuses on understanding the effects of an outer coordination sphere on the performance of molecular catalysts, ultimately aiming to extract the design principles from enzymes for reactions of small molecules such as H<sub>2</sub> and CO<sub>2</sub>.

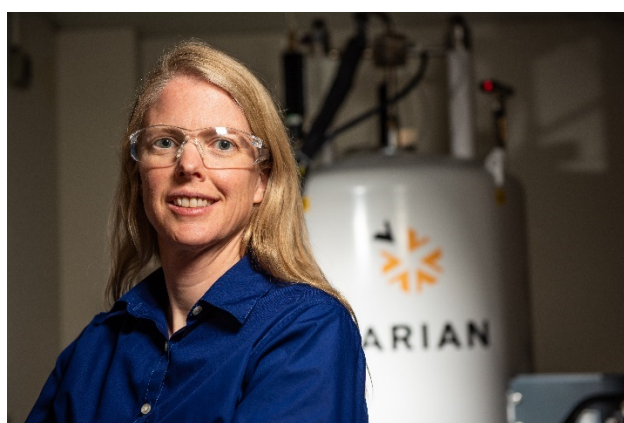


**Table of Contents.** The outer coordination sphere, sometimes called Chicken Fat, is essential for achieving the best catalytic performance for energy transductions.



### Abstract

In order to enable the widespread use of renewable energy from sources such as solar and wind, the energy needs to be stored for use when the renewable sources are not productive. Small molecules such as  $H_2$ ,  $O_2$ ,  $H_2O$ , and  $CO_2$  for example, are excellent storage systems. Nature has evolved machinery, in the form of enzymes, to facilitate these interconversions, allowing the storage and release of electrons when the organism needs to store or release energy. Chemical conversion by metalloenzymes is completed with high selectivity, low energy input, and high

efficiency, all with earth abundant metals and under mild conditions. Although these catalytic properties seem advantageous for industrial use, there are inherent drawbacks to the use of metalloenzymes for industrial applications. However, they provide significant inspiration for developing synthetic complexes that could be implemented broadly. A recent approach in metalloenzyme design has been to focus not only on the atoms immediately attached to the metal, but also the protein scaffold around the active site which has a significant effect on enzymatic catalysis. By taking multiple approaches, the design principles of the protein scaffold are starting to be understood and the essential features required, as well as those not needed, are also being revealed. In this review, we will discuss the effect of organic/peptidic scaffolds, along with medium as an extension of the scaffold, and their varying impacts on catalytic reactivity of energy relevant transformations.

## Introduction

Enzymes are homogeneous catalysts that generally operate with high rates and excellent efficiency under mild conditions, usually ambient temperature and atmospheric pressure. Metalloenzymes are a special class which use a non-precious metal to perform catalytic conversions.<sup>1-4</sup> The efficiencies achieved by enzymes are seldom reproduced with homogeneous synthetic catalysts, even those using precious metals, providing ample evidence that the protein scaffold has a significant contribution to reactivity.<sup>5-7</sup>

The high performance of metalloenzymes is attributed to the highly controlled reactivity achieved via the complex interplay of the metal in the active site, the metal-coordinating atoms, and the dynamics of the protein scaffold that immediately surrounds and extends beyond the active site.<sup>8-15</sup> Bioinorganic research has focused on understanding the structure/functions relationships necessary to achieve this controlled reactivity and recent work has implicated the protein scaffold as having an extremely versatile role in influencing the chemistry of metalloenzymes. While the breadth of effects from the protein scaffold is not fully known, some of the roles of the protein scaffold to directly influence catalytic activity are proposed to include: 1) create favorable interactions between the protein scaffold and the metal/cofactor, 2) position residues and exclude solvent to control the electrostatic environment, 3) embed active sites within pockets to allow access of reactants and limit access of solvent or inhibitors; and 4) allow, or prohibit, conformational changes during the catalytic cycle.

A classic example of the protein environment controlling reactivity through favorable interactions between scaffold and the metal active site is proton channel/relay sites.<sup>16-18</sup> The protein scaffold can have a significant effect on reduction potentials of a metal center, clearly illustrated by the work of Yi Lu's group; the reduction potential of an active site was tuned over a two volt

range requiring only two metals and five mutations. For a given metal, the mutations contributed to approximately 1 V change in redox potential, where the mutations adjusted the hydrogen bonding of amino acid residues surrounding the metal center.<sup>14</sup> The role of the scaffold in slowing O<sub>2</sub> inhibition was demonstrated by Leger and coworkers for NiFe-hydrogenases by making mutations to the channel O<sub>2</sub> uses to reach the active site.<sup>19</sup> Many enzymes are proposed to cycle through an open state and a closed state where large conformational changes allow active site access to enable substrate binding and product removal in the open state, and position residues and substrate for catalysis in the closed state.<sup>20-21</sup> These and other factors all contribute to the control of the enzymatic scaffold on catalytic reactions and enable enzymes to perform very difficult reactions with non-precious metals.

While enzymes can be superior catalysts, because of the difficulty in making them in large quantities, their sensitivity to chemical conditions outside of a narrow range, their small active site to size ratio and in some cases, their instability, enzymes are not currently practical to use on a large scale. Therefore, capturing their features into more robust synthetic systems is ideal. Emphasis continues to be placed on the development of catalysts to store energy from renewable sources, such as solar and wind energies, in chemical bonds.

Synthetically derived organometallic complexes typically rely only on the atoms directly chelating a metal and their substituents (primary coordination sphere; Figure 1) to tune electronic, steric, and in-turn, catalytic properties. We have learned an immense amount from these systems and have a very high level of understanding of how to control the reactivity of a metal by the atoms immediately bound to it. What has become very clear as we have tried to reproduce only the first coordination sphere of enzymes is that this simply is not adequate to reproduce enzymatic

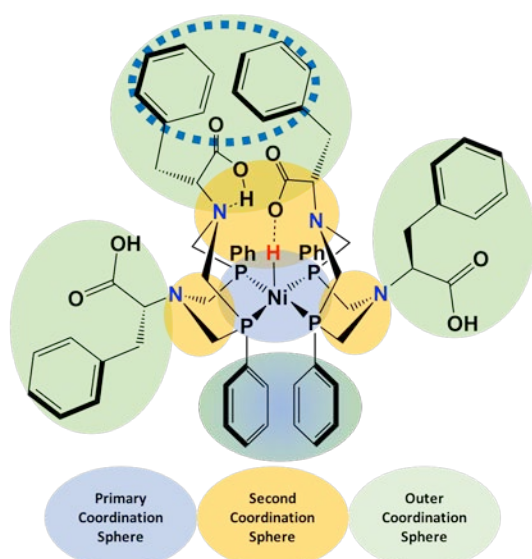


**Figure 1.** Definition of coordination spheres in this paper. The primary coordination sphere (blue) consists of the atoms bound directly to the metal. The second coordination sphere (orange) consists of residues close enough to the metal to directly interact with a bound intermediate, for instance by assisting in hydrogen addition, but not directly binding to the metal. The outer coordination sphere (green) is the rest of the scaffold and can have favorable interactions (dashed blue circle) which can have a variety of effects on catalysis, the topic of this review. Notice that there isn't always a clear delineation between spheres. For instance, the phenyl groups on the phosphorous atoms are typically considered first coordination sphere, but pi-pi stacking, if present, would be an outer coordination sphere effect.

behavior.<sup>6-7, 22-23</sup> Only in the last decade or so have regions beyond the active site been actively pursued as possible components to implement in molecular catalyst design. Many enzymologists break down the enzymatic components relative to catalysis into two spheres: the active site and the second coordination sphere. They refer to the active site as ALL features in the vicinity of catalytic activity as being important to catalysis, independent of whether they are attached to the metal. For instance, in [FeFe]-hydrogenase, the pendant amine would be considered part of the active site while the rest of the protein scaffold is the second coordination sphere. Slightly different definitions have been developed in organometallic complexes to provide an additional level of distinction. These definitions, which follow, will be used throughout this document. Second coordination sphere effects are defined as contributions from atoms near enough to the active

site to influence catalysis but not bound to the active site (Figure 1 and 2). They have received much of this attention, inspired by functional groups observed near metal centers in enzyme crystal



structures. Shown in Figure 2, the family of DuBois catalysts sporting a pendant amine<sup>24</sup> are a well-known example, functionally mimicking the azadithiolate found near the active site of [FeFe]-hydrogenase (Figure 3) which positions a pendant amine next to the iron to aid in H<sub>2</sub> addition and formation.<sup>25-26</sup> Also included in Figure 2, Nocera and coworkers hangman complexes<sup>27-28</sup> and Fujita and coworkers iridium-based complexes,<sup>5, 29-31</sup> which provide additional beautiful examples of the impact of the second coordination sphere.

The rest of the protein scaffold is called the outer coordination sphere (Figure 1) and in principle can have the same contribution to molecular complexes that the protein scaffold of an enzyme has in enzymatic catalysis. A number of synthetic approaches have been taken to capture the effects of the enzymatic scaffold on catalytic activity in synthetic systems (Figure 4). Three general approaches will be discussed in this review: 1) *de novo* “bottom-up” approach (i.e starting with a functional molecular complex and imposing a scaffold), 2) reprogramming non-metal binding protein scaffolds with a molecular complex in a “top-down” approach, and 3) reengineering metal binding proteins (Figure 4). Some excellent examples of mimicking proteins for selectivity have been demonstrated by the groups of Ball<sup>32-33</sup> and Ward,<sup>34</sup> of *de novo* design by the groups of Baker,<sup>35</sup> DeGrado,<sup>36-37</sup> and Pecoraro,<sup>38</sup> and reengineering proteins by the groups of Lombardi and Lu.<sup>39-41</sup> These systems have been covered recently in reviews<sup>38, 42-43</sup> and won’t be considered here. In this review we focus primarily on outer coordination sphere effects on catalysts

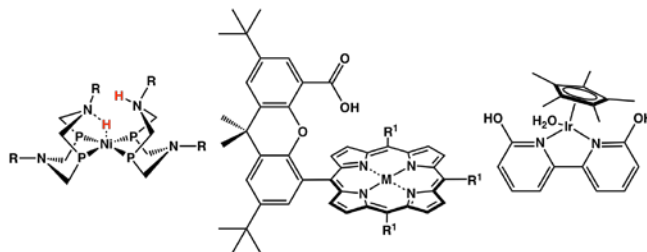


**Figure 2.** Second coordination sphere ligand design for small molecules employs both flexible and rigid functional groups. (A) DuBois-style Ni(P<sub>2</sub>N<sub>2</sub>)<sub>2</sub> complexes are capable of catalyzing both hydrogen oxidation and hydrogen production. (B) hangman style catalyst (Nocera) position CO<sub>2</sub> favorably at the metal center. (C) Ir-Cp\* catalyst favors methanol production by employing a hydroxylated bipyridine ligand (Fujita).

relevant for clean energy applications, with large efforts in conversions of  $H_2$ , growing efforts in conversions of  $CO_2$ , and some work on conversions of  $O_2$  and  $SO_4^{2-}$ .

### Developing Design Principles

While implementing lessons from nature is an obvious strategy, understanding the contribution of the scaffold to the enzyme active site is an ongoing research activity.<sup>44-49</sup> Therefore, it is not always clear which features of the enzyme scaffold are the most important and how much of the scaffold should be captured in a synthetic system. Some common elements that are generally agreed upon include: controlling dynamics to provide positioned functional groups and stabilize the active site, as well as controlling the environment around the active site to influence transition states. We will address complexes which have demonstrated advances in each of these areas.

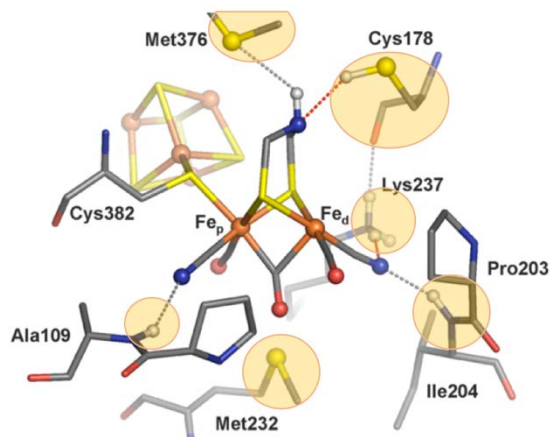


**Figure 3.** Active site H cluster of [FeFe]-hydrogenase (*Clostridium pasteurianum*) showing second coordination sphere stabilization effects, highlighted in orange. The dashed lines show hydrogen bonds indicating outer coordination sphere effects, while the pendant amine, indicated with an arrow, is a second coordination sphere residue and controls hydrogen addition and deprotonation. Reproduced from reference 26. Copyright 2014, Chemical Reviews.

#### *The role of structural dynamics*

Enzymes are known to use dynamics to control reactivity.<sup>50-51</sup> For example, one proposed mechanism for formate dehydrogenase is the dissociation of a selenocysteine residue from the Mo metal center to allow selenium to deprotonate formate and facilitate interconversion of formate to CO<sub>2</sub>.<sup>52-53</sup> Molecular dynamics studies of [FeFe]-hydrogenase suggest structural changes which open a second proton pathway to the active site.<sup>54</sup> Nitrogenase has a large rocking motion connecting the Fe protein and the MoFe protein which triggers electron transfer.<sup>47</sup> Beyond metalloenzymes, adenylate kinases have a hinge like motion which opens an active site to enable reactivity.<sup>55</sup> Small scale motions are also thought to be important, from small vibrations to rocking motions. The later can be more difficult to characterize definitively experimentally, however, computational studies provide very important insight into their potential effects.<sup>47, 56-57</sup> These are

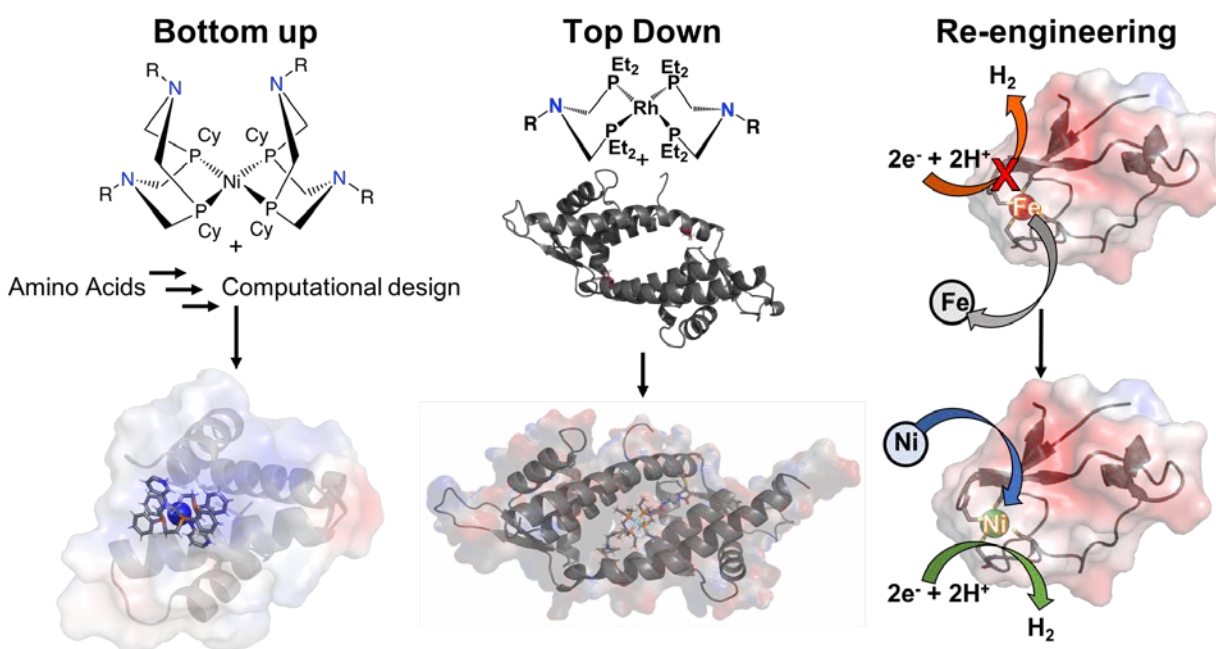


**Figure 4.** Three types of approaches to introducing an outer coordination sphere. The bottom-up approach (left) begins with a molecular complex core with primary and secondary coordination spheres and builds an outer coordination sphere onto that. The top-down approach (center) embeds a defined molecular complex within an ordered scaffold. The reengineering approach (right) replaces a native metal with a foreign metal or introduces a metal binding site.

just some of the many examples demonstrating the importance of controlled motions in enzymatic systems.

Equally as important as having specific controlled motions is restricting or limiting motion resulting in an enforced structure. Restricted motion also exists broadly in biology. For example, in [FeFe]-hydrogenase, Figure 3, the proximal Fe is locked in an octahedral configuration while the distal Fe is maintained as a strict five-coordinate, square pyramidal configuration, where hydrogen bonding interactions of the coordinating ligands to the protein scaffold prevent rearrangement that inactivates the catalyst, best demonstrated by synthetic mimics lacking a protein scaffold which are not able to enforce the structure.<sup>6, 26, 58</sup> Carbon monoxide dehydrogenase (CODH) contains a skewed [4Fe-4S] cubane, allowing the insertion of a Ni atom,<sup>4</sup> while nitrogenase has an extremely rare active site that contains a carbon atom caged between a [4Fe-4S] cluster and a [3Fe2SMo] cluster, better known as FeMo-co, Figure 5.<sup>46, 59-60</sup> Raugei, Seefeldt, and Hoffman combined computational studies and experimentally derived structural and electronic data to show that the second coordination sphere interactions are necessary to stabilize important metal-hydride intermediates and also smoothly facilitate the expansion and contraction of the FeMo-co clusters during the catalytic cycle.<sup>47</sup> Specifically, they were able to show that the protein scaffold enforces an optimal geometry for FeMo-co throughout the entire catalytic cycle, which, contrary to what was previously shown, relies on maintaining metal-hydrides while avoiding protonation of the central

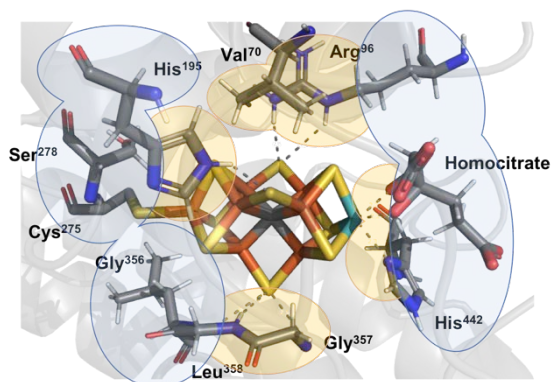


**Figure 5.** Active site of nitrogenase, called FeMo-co, showing second coordination sphere interactions (orange overlay) and outer coordination sphere interactions (blue overlay). Adapted from reference 47. Copyright 2018, Proceedings of the National Academy of Sciences.

carbide that would ultimately lead to CH<sub>4</sub> production and destruction of the FeMo-co cluster.<sup>47, 61-</sup>

63

Shaw, O'Hagan, and co-workers utilize the bottom-up approach to show that the DuBois style catalysts, those containing a pendant amine mimicking [FeFe]-hydrogenase,<sup>66-67</sup> can be decorated with single amino acids, amino acid analogues, or non-biological functional groups to provide significant influence on catalytic performance by controlling structural mobility. Specifically, O'Hagan and coworkers have shown that the catalytic activity of Ni-(bis)diphosphine

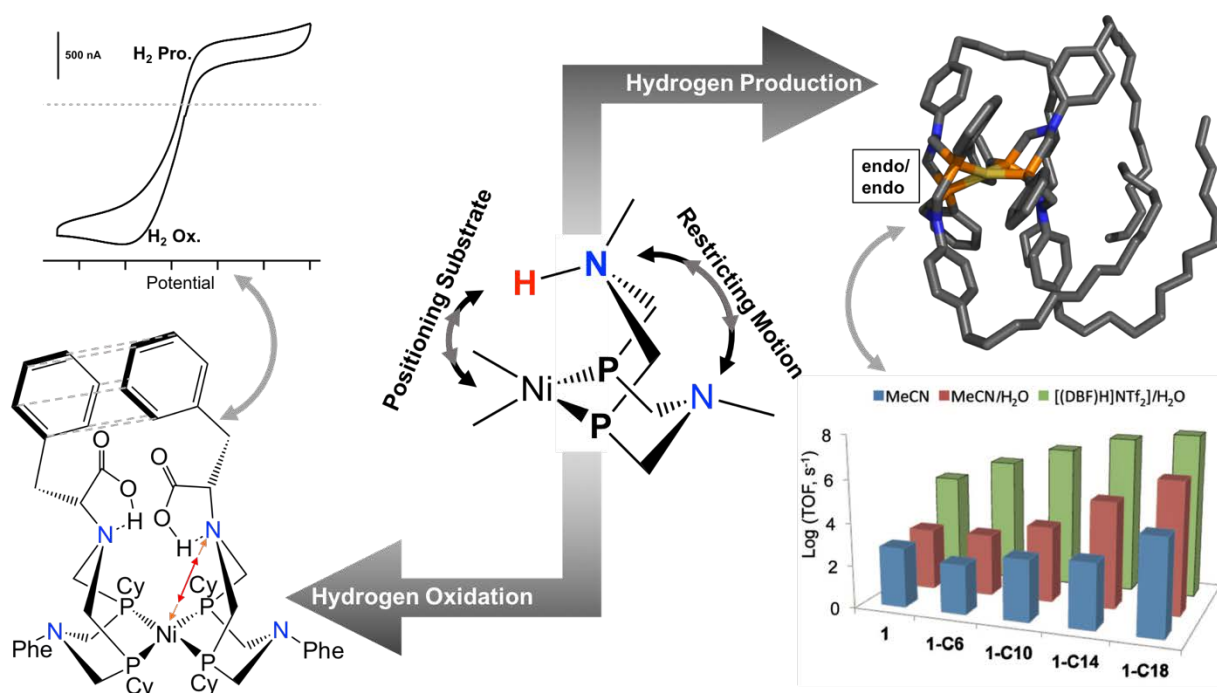


**Figure 6.** Structural dynamics can control small molecular catalysts. In this case a similar restriction of motion benefited H<sub>2</sub> oxidation as well as H<sub>2</sub> production, thought to affect different steps in the catalytic cycle (Center). (Left) Adding amino acids to DuBois style catalysts allows interactions between the COOH groups and the pendant amines as well as between the side chains, which stabilizes the active site conformation. Complexes that have both COOH and side chain interactions such as arginine or phenylalanine have the fastest rates and lowest overpotentials for hydrogen oxidation. The small red arrow shows the Ni to N distance proposed to be altered by the outer coordination sphere to enhance H<sub>2</sub> addition and result in fast rates and reversibility. (Right) Structural dynamics inherent in the DuBois-style catalysts, i.e. isomerization between the endo-endo, endo-exo, and exo-exo conformations, are hindered with the addition of polymer chains attached to the pendant amine, and medium effects also slow this process. Increasing the length of the polymer chain and the viscosity of the solvent resulted in an increase in rate of five orders of magnitude. TOF = turnover frequency. Reproduced with permission from references 64-65. Copyright 2016, Angewandte Chemie International Edition.

derivatives,  $[\text{Ni}(\text{P}^{\text{Ph}}_2\text{N}^{\text{C}_6\text{H}_4\text{R}_2})_2]^{2+}$ , Figure 6, can be dramatically enhanced by controlling the ligand dynamics.<sup>64</sup> Initial studies showed that adding alkyl chains of increasing length ( $n = 6 - 18$ ) increased the turnover frequency (TOF) in acetonitrile-water mixtures of 2000-fold.<sup>68</sup> The hypothesis was that the large groups slowed the boat to chair interconversion of the ring containing the pendant amine, the phosphorous atoms, and the metal (Figure 6), an interconversion demonstrated to result in alternate, inefficient catalytic cycle elements.<sup>65</sup>

There is a correlation between the TOF of the complex and the chair to boat isomerization, suggesting that controlling this dynamic process was responsible for the phenomenal increases in TOF.<sup>64</sup> To test this idea, the team increased the viscosity of the solvent by performing catalysis in acidic ionic liquids, an increase in viscosity of greater than 20-fold, with the assumption that increased viscosity would also slow the interconversion process.<sup>65</sup> A similar trend was observed, where longer chain lengths resulted in faster TOFs, however, this time the TOFs were as fast as  $10^7 \text{ s}^{-1}$ ,<sup>65</sup> several orders of magnitude faster than in acetonitrile, due to the increased viscosity.<sup>65</sup> Further evidence of the role of controlled dynamics was demonstrated by undertaking catalytic experiments in adiponitrile as opposed to acetonitrile.<sup>69</sup> Similar to the acidic ionic liquids, the increased viscosity of the solution had a direct effect on the boat/chair isomerization rate. Leveraging the controlled dynamics achieved by combining the ligand design and the medium viscosity resulted in a catalytic system with reduced overpotential and increased rate, a trend rarely seen in electrocatalytic design. This system illustrates that precise positioning of functional groups often requires complex cooperativity beyond the metal active site, cooperativity not necessarily restricted to interactions within the scaffold, but can be optimized using the medium as well.

Shaw and coworkers also used a bottom-up design with related complexes to result in enhanced catalytic activity in  $\text{H}_2$  oxidation catalysts. In this case, the  $[\text{Ni}(\text{P}^{\text{Cy}_2}\text{N}^{\text{Amino Acid}_2})_2]^{2+}$

derivatives (Figure 6) were used to result in H<sub>2</sub> oxidation activity of up to 10<sup>6</sup> s<sup>-1</sup> at 70 °C, the fastest H<sub>2</sub> oxidation catalysts reported to date, including enzymes, albeit under different conditions.<sup>70</sup> As with the H<sub>2</sub> production catalysts, both attributes within the catalyst and solvent are thought to provide structural stability of the chair-to-boat isomerization (Figure 6).<sup>71</sup> Specifically, it was determined that the amino acid side chains capable of intramolecular interaction slowed chair-to-boat isomerization to enhance catalytic activity.<sup>72</sup> The carboxylic acids also provide stabilization with intramolecular hydrogen bonding, but complexes that had both interacting side chain and COOH groups had slower interconversion and faster rates (Figure 6).<sup>72-</sup><sup>73</sup> Polar solvents were also observed to stabilize the pendant amine in the boat position based on <sup>31</sup>P NMR spectroscopy, keeping the complex in the desired configuration for the most efficient catalytic turnover.<sup>74</sup>

In addition to stabilizing the chair-to-boat isomerization, these catalysts are also proposed to position the pendant amine more optimally for reactivity.<sup>75</sup> This interpretation is based on the observation that the complex is linearly dependent upon H<sub>2</sub> addition, suggesting that H<sub>2</sub> addition is one of the rate determining steps.<sup>70</sup> The addition of H<sub>2</sub> depends upon the distance from the Ni to the N, for both the addition and the heterolytic cleavage steps. Together this data is consistent with the pendant amine being more favorably positioned.<sup>75-76</sup> Crystal structures or more ideally, *operando* characterization with techniques such as XFELS or DTEM would allow direct observation during reactivity. As these methodologies develop, this may allow a more definitive evaluation of the mechanism.

Shafaat and coworkers redesigned a rubredoxin to contain a Ni instead of an Fe (Figure 7) to produce a minimized structural and functional model of [NiFe]-hydrogenase.<sup>78</sup> The resulting Ni-complex shows good activity for electrocatalytic H<sub>2</sub> production, while the Fe complex does not. Further, the active site around the Ni structurally reproduces the geometry of the [NiFe]-hydrogenase.

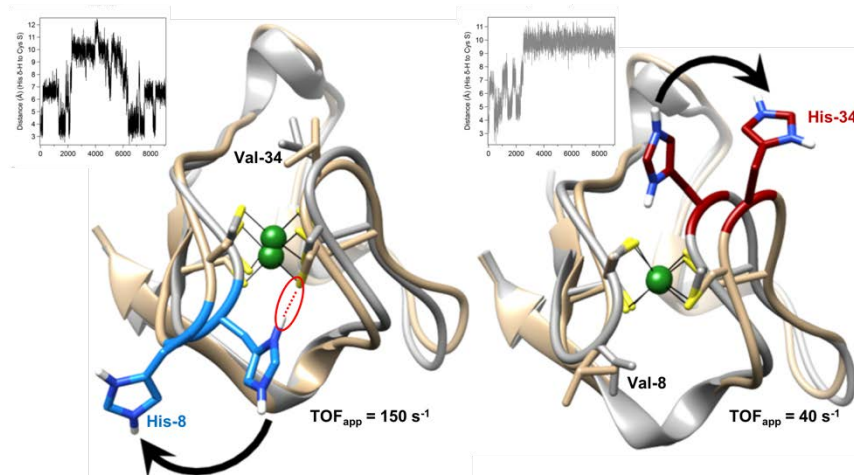


**Figure 7.** Rubredoxin was reengineered by Shafaat and coworkers to reproduce the Ni geometry of [NiFe]-hydrogenase and is active for H<sub>2</sub> production. Modifying valine 8 (left) increased the activity by controlling proton movement and sterics, while (right) the valine 34 to histidine changes the rate limiting step due to the histidine being more solvent exposed, allowing direct protonation of the cysteine. Inset above each structure are the reported distances between the H atom of HisH<sub>2</sub><sup>+</sup> and a coordinating sulfur atom indicating the level of solvent exposure of each histidine; data generated using molecular dynamics simulations. Reproduced with permission from reference 77. Copyright 2018, Journal of the American Chemical Society.

Building on this simple but elegant model, recent studies have focused on implementing computational methods concomitantly with experimental methods to assign vibrational modes and a quantitative assessment of the excited state electronics.<sup>79</sup> Further studies including molecular dynamic simulations, resonance Raman, and quantitative electrochemical analysis, provided a logical pathway to define a reaction mechanism, where a thiol inversion followed by hydride formation was believed to be the rate limiting step.<sup>77</sup> Modulation of the second coordination sphere, by two independent valine to histidine variants, Figure 7, elegantly showed the differential role of the secondary coordination sphere. Here, the V8H construct showed an almost four-fold increase in catalytic activity as compared to the WT, while the V34H variant maintained



comparable activity to the WT. Additionally, the V8H mutant showed TOF's that were independent of pH while the catalytic activity of the V34H mutant was dependent upon pH. The authors suggested that the difference in behavior was due to a change in the rate limiting step from intramolecular (WT and V8H) to intermolecular (V34H) proton transfer. Analysis of molecular dynamics simulations suggests that protonation of the histidine in V8H and V34H results in an opening of catalytic pocket due to a conformational rearrangement by orientation of the protonated histidine(s) away from the active site (Figure 7). In the case of the V34H mutant, solvent and buffer access to the thiolate is increased and allows direct protonation, thus providing a pH dependent mechanism. The increase in TOF for the V8H variant was suggested to be due either to reduced steric strain facilitating proton transfer, or the protonated histidine aiding in proton transfer. This is a great example of the sensitivity of the outer coordination sphere to subtle details of the environment. Even though a single step in the catalytic pathway was the focus, protonation of a cysteine in the primary coordination sphere, similar modifications resulted in very distinct effects.

There has also been a demonstrated impact of controlling dynamics in carbon-based conversions. Fujita and Himeda reported a catalytic system in which paraformaldehyde was converted to methanol in an aqueous medium by Cp\*-Ir complexes bearing aromatic dinitrogen chelating groups.<sup>30</sup> Nine complexes were investigated in this study and the catalyst to perform with the highest TOF and TON employed hydroxide functional groups in the secondary coordination sphere, Figure 8. Density functional theory (DFT) was used to show a direct interaction between the metal and the substrate with concomitant hydrogen bond interactions between the hydroxyl group and substrate. This synergistic interaction between the metal center and the second coordination sphere hydrogen bond interaction was only observed in the catalyst that operated with the highest TON and greatest specificity for methanol production.

Koder and coworkers have demonstrated that the ability of *de novo* designed heme-containing proteins to bind oxygen is affected by the protein dynamics.<sup>80</sup> Specifically, they evaluated two heme's within one protein, one with a conformationally constrained opening due to the loops holding the helices together, and one with a structurally flexible opening away from the loops (Figure 9). The heme near the structurally flexible opening was better able to bind oxygen, even though the helices surrounding each heme are identical. This result was attributed to the increased structural flexibility of one of the histidines near the active site. Making it even more structurally flexible eliminated O<sub>2</sub> binding, thought to be due to increased water accessibility. This data emphasizes the importance of

considering the optimal flexibility of a given system. Understanding the right level of dynamics needed is essential for optimizing protein design.

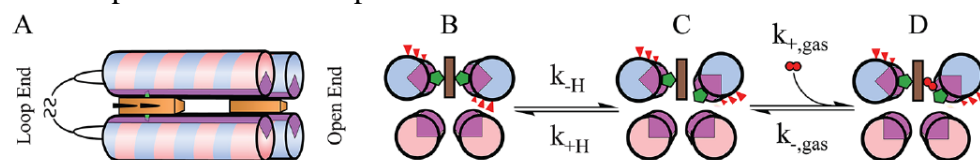


**Figure 9.** *De novo* designed metalloprotein by Koder and co-workers. Both hemes of this artificial metalloprotein have similar environments and binding sites yet display drastically different activity for binding O<sub>2</sub>. (A) The steric hindrance at the loop end and the rotational freedom at the open end are highlighted. (B-D) The rotation of the two helices due to incorporation of three glutamine residues is depicted. The resulting slight conformational change increases solvent exposure and in turn open an O<sub>2</sub> binding site at the heme at the open end. Binding differences were related to the larger degree of flexibility at the open end suggesting that truly rigid structures can be just as damaging to protein function or catalytic activity as too much flexibility. Reproduced with permission from reference 80. Copyright 2013, Biochemistry.

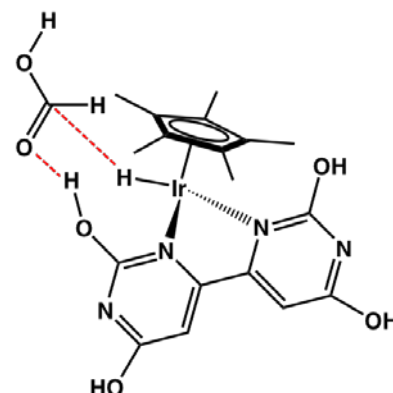


**Figure 8.** Methanol production from formaldehyde using a water-soluble molecular catalyst decorated with hydroxyl groups in the second and outer-coordination sphere. Using DFT, Fujita and co-workers showed that hydrogen bond stabilization of formaldehyde by the hydroxyl groups (dashed red lines) enhanced catalytic activity. Reproduced with permission from reference 30. Copyright 2018, ACS Catalysis.

Borovik and coworkers have recently taken the small molecule mimetic approach for which they are well known<sup>81</sup> and adopted a “top-down” approach by adding these or related complexes into the streptavidin protein environment. In a recent example, they made artificial cupredoxins, using one sulfur atom, modified from the wildtype form, as a ligand. They found that this ligand, along with varying the linker length holding the complex into streptavidin allowed significant alteration of the structural properties of the active site. Using

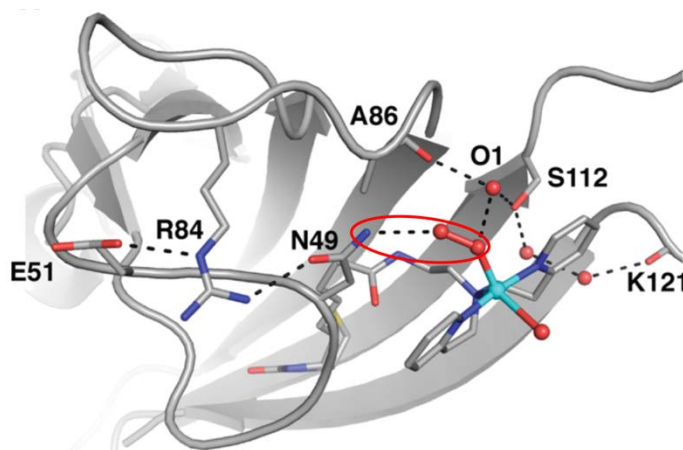


**Figure 10.** Using a top-down approach, biotin was employed as a ligand extension to immobilize a Cu complex within streptavidin. This system demonstrates the power of combining expressed protein scaffolds with synthetic ligand systems to affect chemical structure and reactivity. In this complex, a single hydrogen bond between N49 and a bound dioxygen molecule (shown circled in red) is critical in the oxidation of 4-chlorobenzylamine. Reproduced with permission from reference 82. Copyright 2017, Journal of the American Chemical Society.

a similar approach, but focused on hydrogen bonds, this group was able to demonstrate that a single, well-placed hydrogen bond made the difference between an artificial enzyme that was functional and one that was not (Figure 10).<sup>82</sup> This is an important step in a truly combined synthetic and natural approach where ligands that couldn't be achieved in nature are used in concert with natural ligands.<sup>83</sup>

### *Controlling the environment around the active site*

Controlling the environment around the active site using the protein scaffold can take on many forms and we discuss some of that variety here. It could be controlling electrostatics, hydrogen bonding, excluding water, aiding in substrate addition, or potentially other effects.

Carbon monoxide dehydrogenase, CODH, has a positive charge (lysine) near the active site proposed to stabilize the transition state of  $\text{CO}_2$  to  $\text{CO}$ .<sup>4, 84-87</sup> In nitrogenase, several residues around the active site, including 70Val and  $\alpha$ -195His, have been modified to control the product distribution for  $\text{CO}_2$  reduction, in addition to many of the residues on both faces of the metal cluster

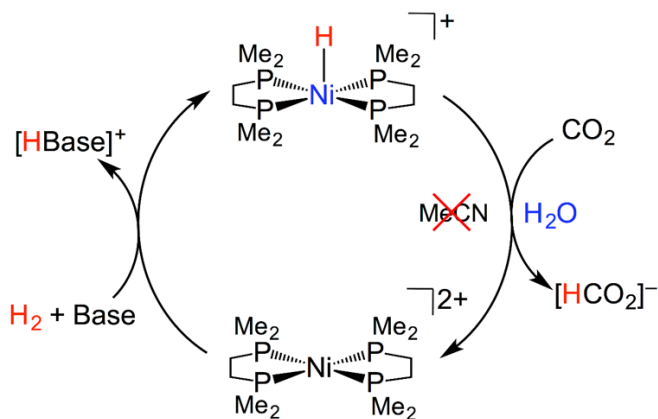


**Figure 11.** The simplest, and maybe most overlooked, “scaffold” or outer coordination sphere influence can be provided by the solvent. In this case the solvent alters the hydricity to either enable or disable  $\text{CO}_2$  activation. Adapted from reference 93. Copyright 2016, Dalton Transactions.

enforcing structure with hydrogen bonding.<sup>47, 63, 88</sup> Multiple metals are another mechanism by which the active site environment can be modulated.<sup>47</sup> In some instances, such as CODH, both metals are actively involved in the transformation. However, in other cases, synergistic cooperation between multi-metallic components is demonstrated, where the conversion happens on only one metal, but the second metal contributes electronic influence on the other metal. Examples of this include [FeFe]-hydrogenase and [NiFe]-hydrogenase, where the distal Fe, furthest from the cubane, is proposed to be the reaction site for [FeFe]-hydrogenase, while the Ni is proposed to be the reaction site for [NiFe]-hydrogenase.<sup>26, 89</sup> Synergistic metal cooperativity is also seen in synthetic systems.<sup>90-91</sup> Recently,  $\text{CO}_2$  hydrogenation was shown by a bi-metallic homogenous catalyst using nickel and gallium prepared by Connie Lu’s group.<sup>92</sup> Catalytic activity was reduced by five orders of magnitude when the gallium was removed from the system, thereby providing evidence that electronic communication and cooperation between two metals during a catalytic cycle is pertinent to efficient chemical transformation.

The simplest way to modulate the environment around the active site is with solvent. Appel and coworkers demonstrate this for  $[\text{HNi}(\text{dmpe})_2]^+$ , a complex which is able to activate  $\text{CO}_2$  in water but not in acetonitrile, a feature which is attributed to the expected change in hydricity in these two solvents (Figure 11).<sup>93</sup> Similarly, Jenny Yang and co-workers provided one of only a handful of published examples of a metal-hydride ( $[\text{HNi}(\text{TMEPE})_2]^+$ ; Figure 12) that was shown to switch from an endergonic to an exergonic process for an identical chemical reaction, solely by changing the solvent of which the chemistry was completed.<sup>94</sup> The measured hydricities for  $[\text{HNi}(\text{TMEPE})_2]^+$  in acetonitrile, dimethylsulfoxide, and water are 50.6, 47.1, and 22.8 kcal/mol, respectively. The hydricities for formate in acetonitrile, dimethylsulfoxide, and water are 44, 42, and 24.1 kcal/mol, respectively. The

$[\text{HNi}(\text{TMEPE})_2]^+$  complex operates at an almost thermoneutral energy level with respect to the hydricity of formate in water. The authors noted that to increase catalytic activity, a more hydritic species is not necessarily the best option as the process is already thermoneutral. An ideal approach would be to increase the kinetics of hydride transfer, presumably by lowering the transition state barrier.

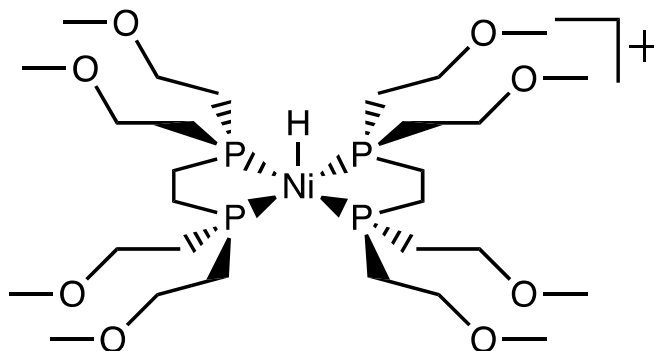


**Figure 12.** Nickel-hydride formed after oxidation of formate in water. Direct outer-coordination sphere effects are observed in this catalyst designed by Yang and co-workers, as the thermodynamic favorability is inverted upon moving from organic solvent to an aqueous medium. Adapted from reference 94. Copyright 2017, Chemical Communications.

The  $\text{Ni}(\text{P}^{\text{R}}_2\text{N}^{\text{R}}_2)_2$  systems also provide examples of controlling reactivity via solvent. For instance, Utschig and her coworkers enabled  $\text{H}_2$  production reactivity in water by associating a  $\text{Ni}(\text{P}_2\text{N}_2)_2$  catalyst to photosystem I.<sup>96</sup> The TOF of the  $\text{Ni}(\text{P}^{\text{Cy}}_2\text{N}^{\text{Arginine}}_2)_2$   $\text{H}_2$  oxidation catalyst was negatively affected by using methanol instead of water as the solvent, where the rate at 70 °C and 100 atm  $\text{H}_2$  dropped by four orders of magnitude (Figure 13).<sup>70</sup> This effect was thought to be due to the significant change in the  $\text{p}K_{\text{a}}$  of the  $\text{COOH}$  group in switching from water ( $\text{p}K_{\text{a}} \sim 3\text{-}4$ ) to methanol ( $\text{p}K_{\text{a}} \sim 20$ ), since this  $\text{COOH}$  group acts as a proton relay. Further, this catalyst was not reversible in methanol while it was in water, perhaps also related to the restricted proton transfer. In another study, a bidirectional/irreversible catalyst,  $\text{Ni}(\text{P}^{\text{Cy}}_2\text{N}^{\text{Pyridizine}}_2)_2$ , was studied in three

solvents: acetonitrile, methanol, or water. Both catalytic potentials lowered in overpotential as more polar solvents were used, moving the catalyst closer to a truly reversible system.<sup>74</sup>

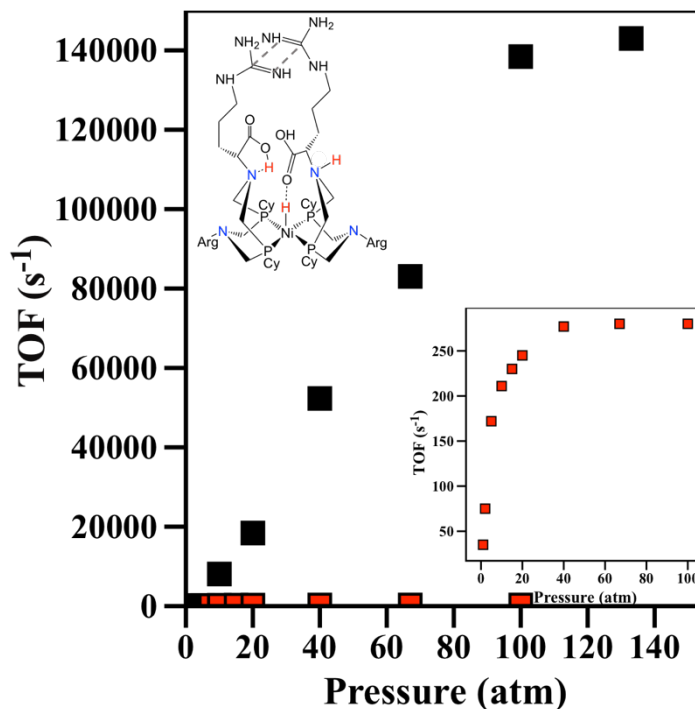


**Figure 13.** Hydrogen oxidation in water by  $[\text{Ni}(\text{P}^{\text{Cy}}_2\text{N}^{\text{Arginine}}_2)_2]$ , black squares, where  $\text{H}_2$  addition contributes to the rate limiting step for  $\text{H}_2$  oxidation. In methanol, the rate limiting step shifts to deprotonation, reducing the TOF by three orders of magnitude (shown in red squares in the main figure, and vertically expanded in the inset). Adapted with permission from reference 95. Copyright 2014, Angewandte Chemie International Edition.

Beyond solvent effects, the control of the active site by a carefully constructed control of the electrostatics is much more reminiscent of the specificity found in enzymes and there is a growing body of literature pointing to the benefit of these groups in synthetic systems. One enzyme-mimetic design strategy is to redesign a natural metal binding motif within a protein to enable specific chemistry, methodology

used very successfully by Yi Lu.<sup>39, 98-99</sup> An excellent example was shown recently, where Lu and coworkers, guided by computational analysis, introduced three cysteine point mutations to cytochrome c peroxidase to position an iron-sulfur cluster below a natively bound heme-cofactor, Figure 14.<sup>97</sup> The computationally designed and experimentally tested artificial enzyme was shown to reduce sulfite, but at a rate of almost 350 times slower when compared to a native sulfite reductase.<sup>100</sup> Further improvements to the scaffold were realized

by three mutations, W51K/H52R/P145K, in the secondary coordination sphere of the heme group to facilitate substrate stabilization interactions, and one mutation, D235C, in the secondary coordination sphere of the [4Fe-4S] cluster. Activity from the W51K/H52R/P145K/D235C construct resulted in a >60-fold increase in catalytic activity, which is 1/5 the rate of the native system.

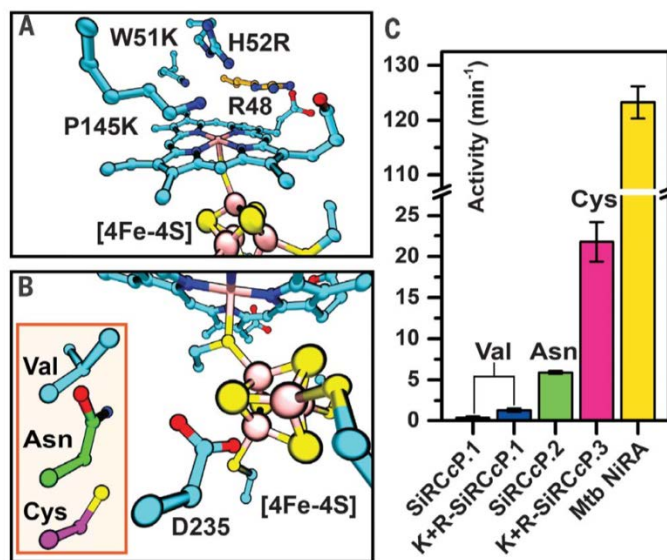


**Figure 14.** Yeast cytochrome C peroxidase (CcP) redesigned as an artificial sulfite reductase (SiRCcP-1) by Lu and co-workers. A) The active site of SiRCcP-1 was computationally designed to mimic the active site of a native sulfite reductase. B) Outer-coordination sphere mutations were introduced that are important for catalytic activity. C) Activity of several mutants of the SiRCcP system compared to the activity of a native sulfite reductase. Reproduced with permission from reference 97. Copyright 2018, Science.

Using a structurally stable protein as a scaffold to introduce a metal has a great deal of precedent from the groups of Lu, Pecararo, and Ball.<sup>14, 33, 42-43</sup> Using a structured protein to introduce a metallocomplex has been explored to some extent, particularly with porphyrins. Lombardi did some early work with horse radish peroxidase mimics<sup>40, 102</sup> and more recently, Roelfes<sup>103-106</sup> has introduced porphyrins into scaffolds to perform chemistries such as cyclopropanation, while Lewis<sup>107-108</sup> used strained cyclo-alkynes to covalently attach a bi-metallic Rh center for olefin cyclopropanation. However, using structured proteins to introduce a functional molecular catalyst is still in its infancy, yet is an approach that holds a lot of promise in developing a mechanistic understanding of the role of the protein scaffold on catalytic activity. In one of the

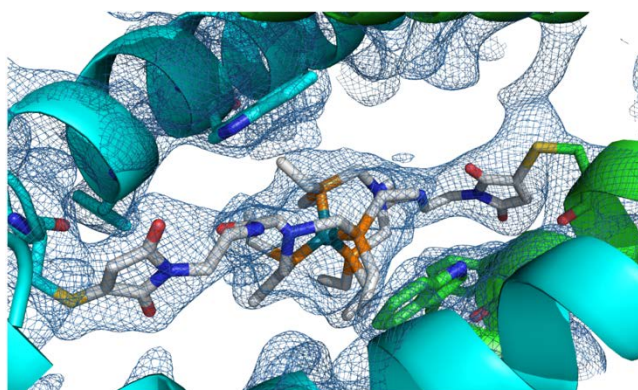


**Figure 15.** Artificial metalloenzyme (PDBID = 6DO0), created using a top down approach, with the molecular complex covalently bound within the cavity created by the homodimeric assembly. This artificial metalloenzyme converts CO<sub>2</sub> to formate at room temperature, yet the complex diffusing alone in solution does not, demonstrating the critical role of the scaffold in activating catalytic activity. Reproduced with permission from reference 101. Copyright 2018, ACS Catalysis.

seminal efforts in this areas, O'Hagan and co-workers used the small, homodimeric protein scaffold (lactococcal multi-drug resistance repressor protein, LmrR from *Lactococcus lactis*) that naturally encodes a pocket that promiscuously binds aromatic and cationic molecules.<sup>101</sup> They introduced a [Rh(PNP)<sub>2</sub>]<sup>+</sup> complex, covalently attached via two maleimide functional groups in the ligand and two cysteines in the scaffold (Figure 15). The resulting Rh-LmrR complex is the first artificial metalloenzyme created from the top

down capable of transforming CO<sub>2</sub> to formate. The complex without the scaffold is not catalytic, demonstrating an important role of the scaffold. Mechanistic studies point to the scaffold aiding



the CO<sub>2</sub> to formate step. Mutagenesis and structural studies are ongoing to understand that role, but there are nearby phenylalanine and tryptophan residues that could be stabilizing CO<sub>2</sub> near the binding site, or a nearby arginine could be stabilizing the CO<sub>2</sub> to formate transition state. An interesting observation with this system is the apparent rearrangement of the catalytic cycle by moving from organic solvent to water, confirmed by <sup>31</sup>P NMR. Similar systems that are active in THF add H<sub>2</sub> to the Rh(I) cation, lose a proton to base, and then convert CO<sub>2</sub> to formate. In water, the mechanism begins similarly via oxidative addition of H<sub>2</sub> to the Rh(I) cation, but in this case it is followed by outer sphere hydride transfer to CO<sub>2</sub>, with deprotonation of the Rh(III)-H as the final step in the catalytic cycle. This example clearly shows the power of a protein scaffold to modulate catalytic activity as only the artificial metalloenzyme was capable of catalytic CO<sub>2</sub> hydrogenation.

In another recent example, Onoda and coworkers demonstrated that nitrobindin (a beta-barrel protein), can be amended to increase the pore size and thereby better accommodate a defined molecular complex (Figure 16).<sup>109</sup> Investigation of the linker length of the ligand framework showed a general trend towards an optimal distance between the metal and the side chain interactions. Specifically, a short one-linker chain which positioned the complex closely within the

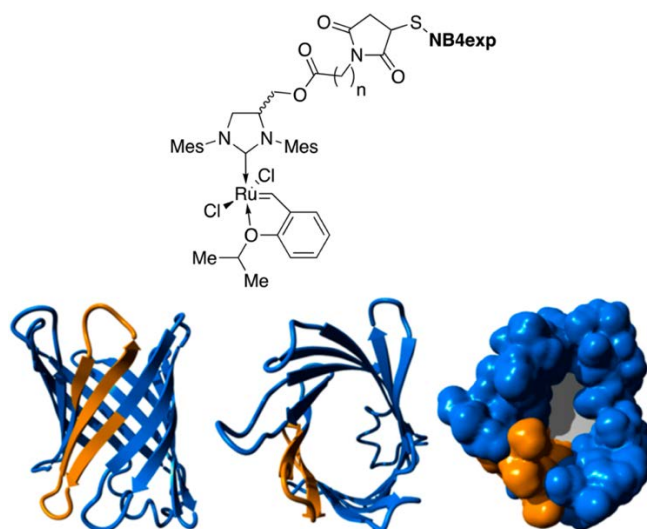


**Figure 16.** Cavity pore size engineering completed by Onoda and co-workers to achieve an optimal positioning of the molecular catalyst within the pore. (Top) Complexes that were investigated are shown, where  $n = 1, 2,$  or  $3$ . (Bottom) Protein structures show the native strands in blue and the engineered portions in orange that accommodated the different complexes. Reproduced with permission from reference 109. Copyright 2018, ACS Catalysis.

cavity was slower than a two-linker chain which positioned it just outside the cavity. However, there was still an impact of the scaffold on olefin metathesis as a three-linker chain, which put the active site away from the cavity, was less active. Specific outer coordination sphere effects are still being identified.

Complexes with a bottom-up style outer coordination sphere have also had an impact on catalysts for CO<sub>2</sub> conversion. Shaw and coworkers investigated a series of Rh(PNP)<sub>2</sub> catalysts with amino acids or dipeptides attached with either Et or Ph on the phosphorous atom (Figure 17). In the case of the Ph-substituted complexes, rates ranging two orders of magnitude were observed depending upon the presence of a pendant amine and what was attached to the pendant amine. For the Et-substituted complexes, only a factor of 5 in rate was observed.

The difference in impact of the second and outer coordination spheres is not easy to explain, particularly when considering the direct comparison of the three complexes studied as either

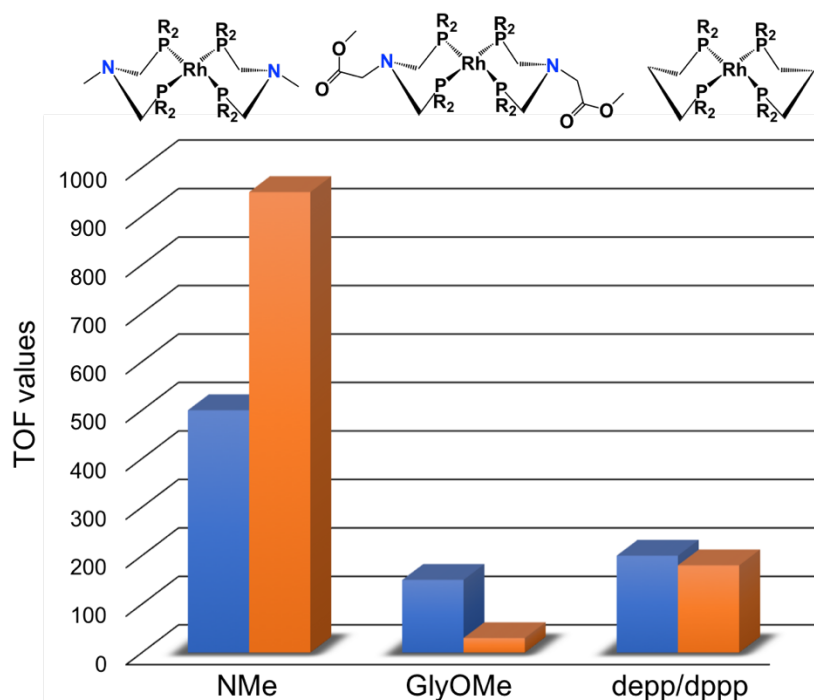


**Figure 17.** Comparison of molecular Rh-bis(diphosphine) catalysts for CO<sub>2</sub> hydrogenation, with ethyl and phenyl substituents shown in blue and orange, respectively. The differences in the relative rates of pairs of CO<sub>2</sub> hydrogenation complexes points to a role of the outer coordination sphere. If the effects were just the primary coordination sphere, i.e. changing from Et to Ph on the phosphorous groups, similar trends would be expected for all three complexes, regardless of presence or absence of an outer coordination sphere. Reproduced with permission from reference 110. Copyright 2018, Faraday Discussions.

the Ph- or Et-substituted. One of the Et-substituted complexes is an order of magnitude faster than the Ph-substituted, one is the same, and one is two times slower (Figure 17). If the difference in the complexes were associated only with the first coordination sphere, each of these would have the same relative trends. That they are different indicates a clear role of the outer coordination sphere. We are currently using advanced computational methods to identify the mechanistic contribution of the outer coordination sphere to this family of catalysts.

Perhaps equally potentially informative in understanding mechanistic implications are cases in which the outer coordination sphere has a minimal impact. For instance, a series of  $\text{Ni}(\text{P}_2\text{N}_2)_2$  complexes for electrochemical oxidation from formate to  $\text{CO}_2$  were substituted with a series of aromatic, aliphatic, and protic dipeptides.<sup>112</sup> The resulting TOF ranged from 2-8  $\text{s}^{-1}$ , with the majority being near 8  $\text{s}^{-1}$ . While it is still not clear why there was so little impact from this series, as we understand the mechanism of the formate oxidation reaction, we will be able to extract the design principles needed for understanding.

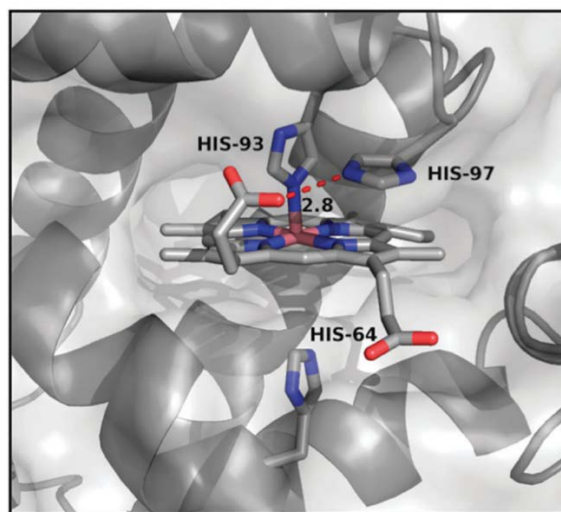


**Figure 18.** Artificial metalloenzyme serving as a functional mimic of hydrogenase by showing electrocatalytic hydrogen production activity. Histidine residues in the second and outer-coordination spheres have a significant impact on catalytic reactivity. Reproduced with permission from reference 111. Copyright 2014, Chemical Communications

Ghirlanda and co-workers reconstituted myoglobin and derivatized it with a cobalt loaded protoporphyrin-IX instead of the native iron system (Figure 18). This re-engineered system was capable of photocatalytic hydrogen production using  $\text{Ru}(\text{bpy})_3$  as a photosensitizer and ascorbate as a sacrificial reductant. Electrocatalytic hydrogen production was also shown at neutral pH.

Modulation of the second and outer coordination spheres was completed by targeting two histidine residues above and below the ring that were exchanged for an alanine, either independently or simultaneously. Substitution of one histidine (His97, Figure 20) led to destabilization of the position of the porphyrin within the pocket and in turn resulted in the lowest catalytic performance in both photo-driven and electrocatalytic-driven system. Conversely, substitution of the second histidine (His64, Figure 18) resulted in the best performing electrocatalytic system. This is likely due to the increased space within the pocket, thereby increasing the access of substrate to the active site. The double mutant performed best under photocatalytic conditions. The specificity and selectivity of the effect of different residues in the outer coordination sphere indicates this was not merely overall charge but that the location of the residues is important and can result in different effects.

#### *The role of specifically positioned functional groups or solvent molecules*

In enzymes, specifically placed functional groups, such as the pendant amine in [FeFe]-hydrogenase or the lysine in CODH, serve a critical role in affecting catalytic activity.<sup>26, 85</sup> Although water is often excluded from the active site, or allowed in only very prescribed ways, waters that are thought to play a specific role are often observed in crystal structures. In [FeFe]-hydrogenase, there is a crystallographic water in the proton pathway. In other proteins, such as cytochrome C oxidase, the waters are thought to compose most of the proton pathway, or water wire.<sup>17</sup>

Dutta and coworkers have just recently showed that positioning a carboxylate group of either phenylalanine or tyrosine near the active site of a Co-Salen complex using a bottom up approach both enables catalysis and provides reversible control of catalysis.<sup>113</sup> In these complexes for H<sub>2</sub> production, at pH values above 4, the carboxylate groups bind the open coordination sites

in the axial positions on the porphyrin, inhibiting catalysis (Figure 19).

Lowering the solution pH to result in a COOH activates catalysis.

Importantly, a complex

without the COOH groups is not functional for catalysis, providing another example of the

scaffold enabling catalysis. The authors suggest that the COOH groups are facilitating proton movement. An analogous catalyst with a non-natural amino acid, tyramine which lacks the COOH group of tyrosine, but contains the phenolic OH group has similar rates and overpotentials. This surprising result is also interpreted as enhancing proton exchange, possibly by building a strong hydrogen bonding network. The similar activity of all three complexes suggests some flexibility in the mechanism of proton transport for this family of complexes.

Using a bottom-up approach, Jones and co-workers used non-canonical amino acids containing a phosphine handle to install four biomimetic diiron clusters in a tripeptide (Figure 20) to produce structural and functional mimics of the [FeFe]-hydrogenase active site.<sup>114</sup> Each construct was shown to be capable of electrocatalytic hydrogen evolution using acetic acid as the proton source, in both neat acetonitrile and a binary solvent of water and acetonitrile. Importantly, in the presence of water, a dramatic increase in catalytic activity was observed, reminiscent of the

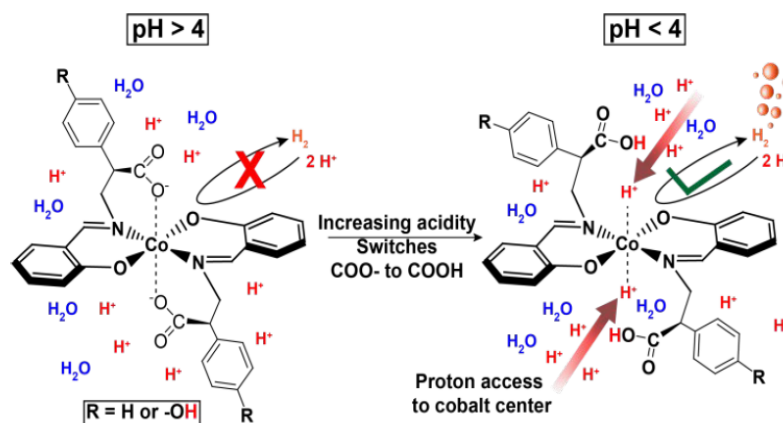


**Figure 19.** Bottom-up approach by Dutta and co-workers where Co-Salen complexes with -COOH or -OH groups were shown to activate catalysis. Specific second coordination sphere interactions were shown to either enable or disable catalytic activity, proposed to be due to protonation of the carboxylic acids facilitating proton transport. Reproduced with permission from reference 113. Copyright 2019, ACS Catalysis.

effect of DuBois style catalysts described above, with a concomitant shift to more positive reduction potentials for the  $\text{Fe}^{\text{I}}\text{Fe}^{\text{I}}/\text{Fe}^{\text{I}}\text{Fe}^0$  transitions. Here, the peptide provided an increased overall polarity to complex, allowing electrocatalytic investigation in partially aqueous medium. The presence of water resulted in an anodic shift in the first reduction event, and a dramatic increase in the observed electrocatalytic current. It should also be noted that the most active species was one that contained both a phenyl bridge between the diiron clusters, as well as a phenyl phosphine species (Figure 20). It is possible that the phenyl

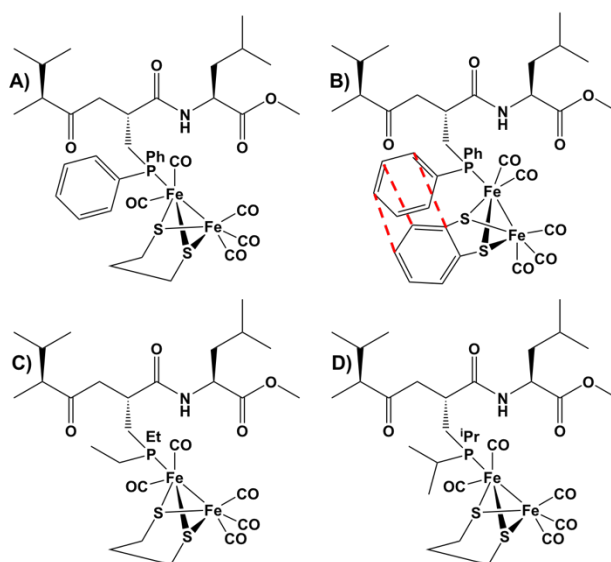


**Figure 20.** Structural and functional biomimetic diiron clusters, designed by Jones and co-workers to mimic  $[\text{FeFe}]$  hydrogenase, are installed directly on solid phase synthesized peptides containing phosphine based non-canonical amino acids. Complex B proved to be the most catalytically competent construct. Interestingly, B is the only construct to have an obvious outer coordination sphere interaction between the aryl-bridging dithiolate and the aryl rings of the phenyl-phosphine, while A, C, D do not. Reproduced with permission from reference 114. Copyright 2015, Dalton Transactions.

dithiolate bridge was positioning the Fe-Fe cluster, via  $\pi$ - $\pi$  stacking, to favorably interact with the second and outer coordination sphere of the peptide scaffold. They are still identifying the specific interactions that are contributing from the outer coordination sphere, but the observation of activity is a significant advance over previous models.<sup>115</sup>

Artero and coworkers have compared the effect of the scaffold of two different heme oxygenase proteins on a cobaloxime (Figure 21). Inserting cobaloxime into these oxygenase's results in up to five-fold increases relative to cobaloxime alone or myoglobin. A serine residue and a lysine residue are attributed to providing an open and closed active site and are the topic of further studies to investigate the role of the scaffold.<sup>116</sup>

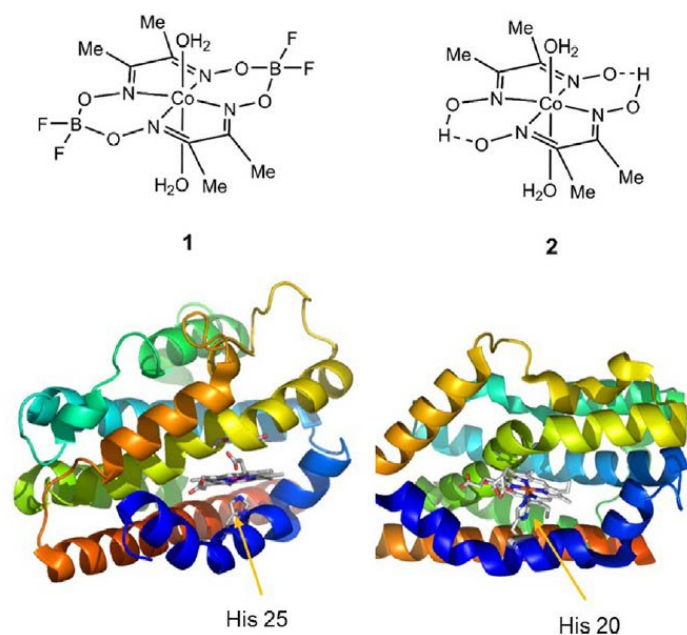


**Figure 21.** Using a reengineering approach Artero and co-workers inserted one of two cobaloximes in place of heme in the binding site of heme oxygenase and myoglobin to produce functional mimics of hydrogen producing hydrogenase enzymes. Reproduced with permission from reference 116. Copyright 2016, ChemPlusChem.

this amine would be interesting to test to see if better (or possibly worse) impacts on catalytic performance could be achieved.

In molecular catalysts, solvent molecules can play a specific role beyond just changing thermodynamic properties as discussed above. In an  $O_2$  reduction catalyst, the Fe-porphyrin with a pendant pyridyl groups was proposed to have a series of ordered

Using an iron complex, Figure 22, controlling proton movement with an outer coordination sphere pendant amine in a bottom-up approach resulted in faster rates with no increase in overpotential for  $H_2$  oxidation.<sup>117</sup>

$(Cp^{C5F4N})Fe(P^{Et}N^{(CH_2)_3NM_2}P^{Et})(Cl)$  showed that an outer coordination sphere amine enhanced catalysis by as much as an order of magnitude relative to the complex without the outer coordination sphere amine.<sup>117</sup> The flexible nature of

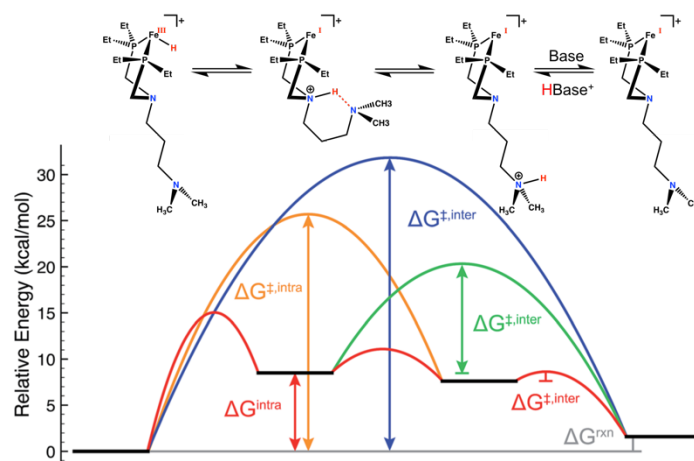


**Figure 22.** Helm and co-workers included an amine in the outer coordination sphere of an Fe-diphosphine complex that provided a 10-fold increase in TOF for hydrogen oxidation, with only a 10 mV increase in overpotential. The different barriers show the contribution of each step relative to the overall catalytic reaction. Reproduced with permission from reference 117. Copyright 2015, Chemical Science.

waters around the pyridinium ions and around the O<sub>2</sub> ligand, helping to facilitate proton delivery.<sup>118</sup> Further related studies demonstrated that medium effects affected catalytic performance more significantly than intentional modifications in the second coordination sphere of the catalyst.<sup>119</sup>

In the Ni(P<sup>R</sup><sub>2</sub>N<sup>R</sup><sub>2</sub>)<sub>2</sub> H<sub>2</sub> production and oxidation catalysts, a very significant, and different role of water was observed. For H<sub>2</sub> production catalysts, small amounts of water enhanced the rate by up to 50 fold.<sup>120-123</sup> This was shown to be a contribution of several factors. The first was assisting proton delivery or removal to the nickel through the pendant amine from the bulk solvent.<sup>124</sup> It was also predicted to limit the exo pinched structure (Figure 6), preventing inefficient catalytic cycles.<sup>64</sup> Also, as indicated above, water stabilized the endo structure preferentially over the exo structure, positioning the pendant amine in the desired position throughout the cycle.<sup>74</sup> Therefore the water had influence in the second and outer coordination spheres.

For Ni(P<sup>R</sup><sub>2</sub>N<sup>R</sup><sub>2</sub>)<sub>2</sub> H<sub>2</sub> oxidation catalysts, the effect was equally as impressive, but this time, water affected the overpotential, rather than the TOF. This was proposed to be due to changing the ability of the complex to deprotonate before the first oxidation in the presence of water, shifting the onset potential by as much as 300 mV.<sup>125-127</sup>

While placing pendant amines in the second coordination sphere has been well-established to have a positive impact on catalysis, the effect of additional relays has been less studied. Ni(P<sup>R</sup><sub>2</sub>N<sup>R</sup><sub>2</sub>)<sub>2</sub> complexes with additional functional groups including amides, esters, amines, ethers, and COOH acid groups showed enhanced proton transport and enhanced catalytic properties with these added groups.<sup>72-73, 75, 95, 125, 128-130</sup> Reduction of overpotential was the most significant effect, although under the right conditions, rates were also enhanced. In some cases, these functional groups enabled reversibility, though more work is needed to understand the details of why some



of the groups resulted in reversibility and some did not. We predict that it was more than just the  $pK_a$ , including additional features such as proper positioning of the pendant amine and rate of  $H_2$  addition.<sup>72-73</sup>

Pecoraro and coworkers recently showed the first direct demonstration of water being exchanged at the nanosecond scale using perturbed angular correlation.<sup>132</sup> Exchange of water to and from the cysteine coordinated  $Cd^{2+}$  metal site was observed with a triple-helix *de novo* designed protein, Figure 23, observing the  $CdS_3$  and  $CdS_3OH_2$  species. The observation of this process has broad implications for catalysis in general, but particularly relevant to the topic of this review is the effect of a leucine to alanine substitution  $\sim 10$  Å away. Each of the peptide chains in the triple helix has the sequence Ac-G(LKALEEK)<sub>4</sub>. Replacing this leucine did not measurably affect the structure of the

$CdS_3$  active site, however, the equilibrium constant shifted to favor the complex with water disassociated, and the residence time of the water on the  $Cd^{2+}$  metal center decreased by as much as 20% and may

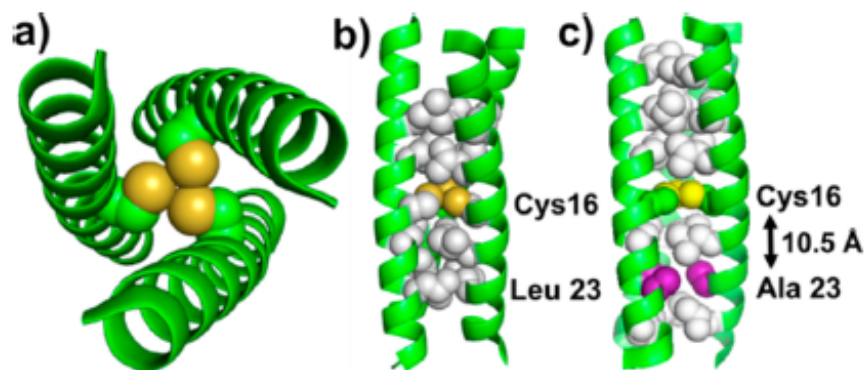


**Figure 23.** Pecoraro and co-workers designed an artificial metalloprotein consisting of a triple-helix that binds  $Cd^{2+}$ . The metal binding site is depicted in A). B) Model of the apo-protein with leucine residues shown as white spheres. C) Substitution of an outer-coordination sphere residue, alanine for leucine at position 23 10 Å away, produces a change in exchange rate and equilibrium constant of a water ligand, possibly due to a destabilized, water-bound structure. Reproduced with permission from reference 131. Copyright 2016, Journal of the American Chemical Society.

point to a destabilized structure with water associated. This exciting direct measurement of the

impact of a distant residue on active site ligand disassociation is strong evidence of how important it is to consider the outer coordination sphere.

Artero and coworkers showed that installation of a DuBois style  $P_2N_2$  to a molecular cobalt complex produces catalysts capable of electrocatalytic transformation of carbon dioxide to formate in a binary solvent of DMF and water at room temperature and atmospheric pressure (Figure 24).<sup>133</sup>

Removing water and replacing it with a soluble base, redirected the faradaic yield to favor hydrogen evolution by an order of magnitude (5% to 50%), and a two-fold decrease in faradaic yield for formic acid production. The complexes were equally stable in the presence and absence of water, however, the activity in the presence of base is  $< 1 s^{-1}$ , dramatically reduced from the rate of  $150 s^{-1}$  in the presence of water. Computational analysis provided the hypothesis that the amine group in the  $P_2N_2$  ligand is responsible for promoting hydrogen bonding interactions between the ligand, water,

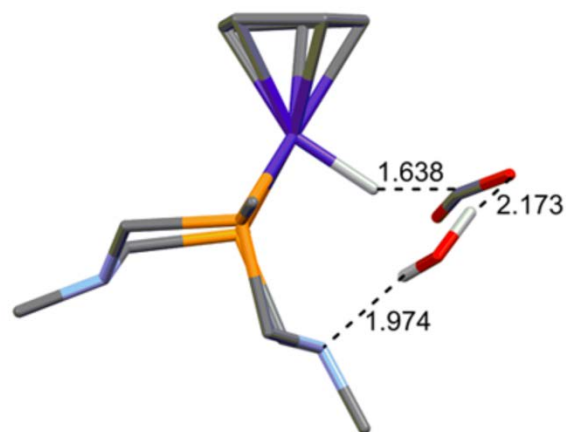


**Figure 24.** A molecular cobalt complex capable of electrocatalytic conversion of  $CO_2$  to formate showing a favorable interaction between the second coordination sphere of the amine of a  $P_2N_2$  ligand, water, and carbon dioxide facilitating the conversion of  $CO_2$  to formate under ambient conditions. Reproduced with permission from reference 133. Copyright 2017, Journal of the American Chemical Society.

and  $CO_2$ , highlighting a potential beneficial interplay between precisely positioned second coordination sphere ligand interactions, the surrounding solvent, and a specific substrate.

## Conclusions

Over the past decade, many researchers have contributed to arrive at a clear conclusion: the second and outer coordination spheres of molecular complexes can be as important to synthetic complexes as they are to enzymes. There are many different forms of influence. Here we identified key roles that include: controlled structural motions, an influence of the electrostatic environment, controlling hydrogen bonding, and precisely placed water or other functional groups to move protons. It is likely that the mechanisms of at least some of these systems are much more complex than our current interpretations, and the effect may ultimately be entirely different as our understanding of the mechanistic impact of the outer coordination sphere becomes more sophisticated. One thing is clear: because the outer coordination spheres of enzymes are not completely understood, the natural result is that the synthetic systems sometimes inform the enzymatic systems, although as highlighted here, in many cases, we do not completely understand the effect of the outer coordination sphere. The effects of the outer coordination sphere are necessarily coupled to those of the active site, often creating a challenge in proposing and testing a mechanism. Yet as we continue to push the forefront using both enzymes and synthetic catalysts and developing new experimental and computational technologies, we will continue to enhance our understanding of the basic components needed to achieve fast, efficient, selective and specific catalysis that will enable a clean energy future.

## Conflicts of Interest

There are no conflicts of interest to declare.

## Acknowledgements

This review highlights previously published work supported by the Office of Science Early Career Research Program through the US Department of Energy (DOE), Basic Energy Sciences (BES); US DOE BES, Chemical Sciences, Geoscience and Bioscience; and the Center for Molecular Electrocatalysis, an Energy Frontier Research Center funded by the U.S. DOE, Office of Science, BES. Pacific Northwest National Laboratory PNNL is operated by Battelle for the US DOE.

## References

1. Waldron, K. J.; Rutherford, J. C.; Ford, D.; Robinson, N. J., Metalloproteins and metal sensing. *Nature* **2009**, *460* (7257), 823-830.
2. Shafaat, H. S.; Rüdiger, O.; Ogata, H.; Lubitz, W., [NiFe] hydrogenases: A common active site for hydrogen metabolism under diverse conditions. *BBA - Bioenergetics* **2013**, *1827* (8-9), 986-1002.
3. Boer, J. L.; Mulrooney, S. B.; Hausinger, R. P., Nickel-dependent metalloenzymes. *Arch Biochem Biophys* **2014**, *544*, 142-152.
4. Can, M.; Armstrong, F. A.; Ragsdale, S. W., Structure, function, and mechanism of the nickel metalloenzymes, CO dehydrogenase, and acetyl-CoA synthase. *Chem Rev* **2014**, *114* (8), 4149-74.
5. Wang, W.-H.; Himeda, Y.; Muckerman, J. T.; Manbeck, G. F.; Fujita, E., CO<sub>2</sub> hydrogenation to formate and methanol as an alternative to photo- and electrochemical CO<sub>2</sub> reduction. *Chem Rev* **2015**, *115* (23), 12936-12973.
6. Gloaguen, F.; Rauchfuss, T. B., Small molecule mimics of hydrogenases: hydrides and redox. *Chem Soc Rev* **2009**, *38*, 100-108.
7. Caserta, G.; Roy, S.; Atta, M.; Artero, V.; Fontecave, M., Artificial hydrogenases: biohybrid and supramolecular systems for catalytic hydrogen production or uptake. *Curr Opin Chem Biol* **2015**, *25*, 36-47.
8. Al-Attar, S.; de Vries, S., Energy transduction by respiratory metallo-enzymes: From molecular mechanism to cell physiology. *Coordin Chem Rev* **2013**, *257* (1), 64-80.
9. Holm, R. H.; Kennepohl, P.; Solomon, E. I., Structural and functional aspects of metal sites in biology. *Chem Rev* **1996**, *96*, 2239-2314.
10. Dawson, J. H., Probing structure-function relations in heme-containing oxygenases and peroxidases. *Science* **1988**, *240*, 433-439.
11. Armstrong, R. N., Structure-function relationships in enzymic catalysis. Can chimeric enzymes contribute? *Chem Rev* **1990**, *90*, 1309-1325.
12. Ross, M. R.; White, A. M.; Yu, F.; King, J. T.; Pecoraro, V. L.; Kubarych, K. J., Histidine orientation modulates the structure and dynamics of a de novo metalloenzyme active site. *J Am Chem Soc* **2015**, *137* (32), 10164-10176.

13. Warshel, A.; Sharma, P. K.; Kato, M.; Xiang, Y.; Liu, H.; Olsson, M. H. M., Electrostatic basis for enzyme catalysis. *Chem Rev* **2006**, *106*, 3210-3235.
14. Hosseinzadeh, P.; Marshall, N. M.; Chacón, K. N.; Yu, Y.; Nilges, M. J.; New, S. Y.; Tashkov, S. A.; Blackburn, N. J.; Lu, Y., Design of a single protein that spans the entire 2-V range of physiological redox potentials. *Proc Natl Acad Sci USA* **2016**, *113* (2), 262-267.
15. Low, D. W.; Hill, M. G., Rational fine-tuning of the redox potentials in chemically synthesized rubredoxins. *J Am Chem Soc* **1998**, *120*, 11536-11537.
16. Smith, M. A.; Majer, S. H.; Vilbert, A. C.; Lancaster, Kyle M., Controlling a burn: outer-sphere gating of hydroxylamine oxidation by a distal base in cytochrome P460. *Chem Sci* **2019**, *10* (13), 3756-3764.
17. Wraight, C. A., Chance and design - proton transfer in water, channels and bioenergetic proteins. *Biochim Biophys Acta* **2006**, *1757*, 886-912.
18. Cui, Q.; Karplus, M., Is a "proton wire" concerted or stepwise - A model study of proton transfer in carbonic anhydrase. *J Phys Chem B* **2003**, *107*, 1071-1078.
19. Liebgott, P.-P.; Leroux, F.; Burlat, B.; Dementin, S.; Baffert, C.; Lautier, T.; Fourmond, V.; Ceccaldi, P.; Cavazza, C.; Meynial-Salles, I.; Soucaille, P.; Fontecilla-Camps, J. C.; Guigliarelli, B.; Bertrand, P.; Rousset, M.; Léger, C., Relating diffusion along the substrate tunnel and oxygen sensitivity in hydrogenase. *Nat Chem Biol* **2009**, *6*, 63.
20. Bohl, T. E.; leong, P.; Lee, J. K.; Lee, T.; Kankanala, J.; Shi, K.; Demir, O.; Kurahashi, K.; Amaro, R. E.; Wang, Z.; Aihara, H., The substrate-binding cap of the UDP-diacetylglucosamine pyrophosphatase LpxH is highly flexible, enabling facile substrate binding and product release. *J Biol Chem* **2018**, *293* (21), 7969-7981.
21. Cherney, M. M.; Bowler, B. E., Protein dynamics and function: Making new strides with an old warhorse, the alkaline conformational transition of cytochrome c. *Coord Chem Rev* **2011**, *255* (7-8), 664-677.
22. Shaw, W. J.; Helm, M. L.; DuBois, D. L., A modular, energy-based approach to the development of nickel containing molecular electrocatalysts for hydrogen production and oxidation. *BBA - Bioenergetics* **2013**, *1827* (8-9), 1123-1139.
23. Ginovska-Pangovska, B.; Dutta, A.; Reback, M. L.; Linehan, J. C.; Shaw, W. J., Beyond the active site: The impact of the outer coordination sphere on electrocatalysts for hydrogen production and oxidation. *Acc Chem Res* **2014**, *47* (8), 2621-2630.
24. Dubois, D. L., Development of molecular electrocatalysts for energy storage. *Inorg Chem* **2014**, *53* (8), 3935-3960.
25. Reijerse, E. J.; Pham, C. C.; Pelmeshnikov, V.; Gilbert-Wilson, R.; Adamska-Venkatesh, A.; Siebel, J. F.; Gee, L. B.; Yoda, Y.; Tamasaku, K.; Lubitz, W.; Rauchfuss, T. B.; Cramer, S. P., Direct observation of an iron-bound terminal hydride in [FeFe]-hydrogenase by nuclear resonance vibrational spectroscopy. *J Am Chem Soc* **2017**, *139* (12), 4306-4309.
26. Lubitz, W.; Ogata, H.; Rüdiger, O.; Reijerse, E., Hydrogenases. *Chem Rev* **2014**, *114* (8), 4081-4148.
27. Bediako, D. K.; Solis, B. H.; Dogutan, D. K.; Roubelakis, M. M.; Maher, A. G.; Lee, C. H.; Chambers, M. B.; Hammes-Schiffer, S.; Nocera, D. G., Role of pendant proton relays and proton-coupled electron transfer on the hydrogen evolution reaction by nickel hangman porphyrins. *Proc Natl Acad Sci USA* **2014**, *111* (42), 15001-15006.

28. Dogutan, D. K.; Bediako, D. K.; Teets, T. S.; Schwalbe, M.; Nocera, D. G., Efficient synthesis of hangman porphyrins. *Org Lett* **2010**, *12* (5), 1036-1039.
29. Small, Y. A.; DuBois, D. L.; Fujita, E.; Muckerman, J. T., Proton management as a design principle for hydrogenase-inspired catalysts. *Energy Environ Sci* **2011**, *4* (8), 3008.
30. Wang, L.; Ertem, M. Z.; Murata, K.; Muckerman, J. T.; Fujita, E.; Himeda, Y., Highly efficient and selective methanol production from paraformaldehyde and water at room temperature. *ACS Catal* **2018**, *8* (6), 5233-5239.
31. Wang, W.-H.; Hull, J. F.; Muckerman, J. T.; Fujita, E.; Himeda, Y., Second-coordination-sphere and electronic effects enhance iridium(iii)-catalyzed homogeneous hydrogenation of carbon dioxide in water near ambient temperature and pressure. *Energy Environ Sci* **2012**, *5* (7), 7923.
32. Ohata, J.; Ball, Z. T., Rhodium at the chemistry-biology interface. *Dalton Trans* **2018**, *47* (42), 14855-14860.
33. Ball, Z. T., Designing enzyme-like catalysts: A rhodium(II) metalloprotein case study. *Acc Chem Res* **2012**, *46* (2), 560-570.
34. Ward, T. R., Artificial metalloenzymes based on the biotin-avidin technology: enantioselective catalysis and beyond. *Acc Chem Res* **2011**, *44*, 47-57.
35. Huang, P. S.; Boyken, S. E.; Baker, D., The coming of age of de novo protein design. *Nature* **2016**, *537* (7620), 320-7.
36. Di Costanzo, L.; Wade, H.; Geremia, S.; Randaccio, L.; Pavone, V.; DeGrado, W. F.; Lombardi, A., Toward the de novo design of a catalytically active helix bundle: a substrate-accessible carboxylate-bridged dinuclear metal center. *J Am Chem Soc* **2001**, *123*, 12749-12757.
37. Kaplan, J.; DeGrado, W. F., De novo Design of Catalytic Proteins. *Proc Natl Acad Sci USA* **2004**, *101* (32), 11566-11570.
38. Zastrow, M. L.; Pecoraro, V. L., Designing functional metalloproteins: from structural to catalytic metal sites. *Coordin Chem Rev* **2013**, *257* (17-18), 2565-2588.
39. Hosseinzadeh, P.; Lu, Y., Design and fine-tuning redox potentials of metalloproteins involved in electron transfer in bioenergetics. *BBA - Bioenergetics* **2016**, *1857* (5), 557-581.
40. Lombardi, A.; Natri, F.; Pavone, V., Peptide-based heme-protein models. *Chem Rev* **2001**, *101*, 3165-3189.
41. Maglio, O.; Natri, F.; Rosales, R. T. M. d.; Faiella, M.; Pavone, V.; DeGrado, W. F.; Lombardi, A., Diiron-containing metalloproteins: developing functional models. *C R Chimie* **2007**, *10*, 703-720.
42. Shaw, W. J., The Outer-Coordination Sphere: Incorporating Amino Acids and Peptides as Ligands for Homogeneous Catalysts to Mimic Enzyme Function. *Cataly Rev* **2012**, *54* (4), 489-550.
43. Yu, F.; Cangelosi, V. M.; Zastrow, M. L.; Tegoni, M.; Plegaria, J. S.; Tebo, A. G.; Mocny, C. S.; Ruckthong, L.; Qayyum, H.; Pecoraro, V. L., Protein design: Toward functional metalloenzymes. *Chem Rev* **2014**, *114* (7), 3495-3578.
44. Berggren, G.; Adamska, A.; Lambertz, C.; Simmons, T. R.; Esselborn, J.; Atta, M.; Gambarelli, S.; Mouesca, J. M.; Reijerse, E.; Lubitz, W.; Happe, T.; Artero, V.; Fontecave, M., Biomimetic assembly and activation of [FeFe]-hydrogenases. *Nature* **2013**, *498* (7456), 66-69.

45. Esselborn, J.; Lambertz, C.; Adamska-Venkatesh, A.; Simmons, T.; Berggren, G.; Noth, J.; Siebel, J.; Hemschemeier, A.; Artero, V.; Reijerse, E.; Fontecave, M.; Lubitz, W.; Happe, T., Spontaneous activation of [FeFe]-hydrogenases by an inorganic [2Fe] active site mimic. *Nature* **2013**, *9* (10), 607-609.
46. Keable, S. M.; Zadvornyy, O. A.; Johnson, L. E.; Ginovska, B.; Rasmussen, A. J.; Danyal, K.; Eilers, B. J.; Prussia, G. A.; LeVan, A. X.; Raugei, S.; Seefeldt, L. C.; Peters, J. W., Structural characterization of the P(1+) intermediate state of the P-cluster of nitrogenase. *J Biol Chem* **2018**, *293* (25), 9629-9635.
47. Raugei, S.; Seefeldt, L. C.; Hoffman, B. M., Critical computational analysis illuminates the reductive-elimination mechanism that activates nitrogenase for N<sub>2</sub> reduction. *Proc Natl Acad Sci USA* **2018**, *115* (45), E10521-E10530.
48. Abou Hamdan, A.; Dementin, S.; Liebgott, P.-P.; Gutierrez-Sanz, O.; Richaud, P.; De Lacey, A. L.; Rousset, M.; Bertrand, P.; Cournac, L.; Léger, C., Understanding and tuning the catalytic bias of hydrogenase. *J Am Chem Soc* **2012**, *134* (20), 8368-8371.
49. Morra, S.; Maurelli, S.; Chiesa, M.; Mulder, D. W.; Ratzloff, M. W.; Giamello, E.; King, P. W.; Gilardi, G.; Valetti, F., The effect of a C298D mutation in CaHydA [FeFe]-hydrogenase: Insights into the protein-metal cluster interaction by EPR and FTIR spectroscopic investigation. *BBA - Bioenergetics* **2016**, *1857* (1), 98-106.
50. Boehr, D. D.; Dyson, H. J.; Wright, P. E., An NMR perspective on enzyme dynamics. *Chem Rev* **2006**, *106*, 3055-3079.
51. Meyer, M. P.; Tomchick, D. R.; Klinman, J. P., Structure and dynamics affect hydrogen tunneling- The impact of a remote side chain (I553) in soybean lipoxygenase-1. *Proc Natl Acad Sci USA* **2008**, *105*, 1146-1151.
52. Leopoldini, M.; Chiodo, S. G.; Toscano, M.; Russo, N., Reaction mechanism of molybdoenzyme formate dehydrogenase. *Chem Eur J* **2008**, *14* (28), 8674-8681.
53. Boyington, J. C.; Gladyshev, V. N.; Khangulov, S. V.; Stadtman, T. C.; Sun, P. D., Crystal structure of formate dehydrogenase H: catalysis involving Mo, molybdopterin, selenocysteine, and an Fe<sub>4</sub>S<sub>4</sub> cluster. *Science* **1997**, *275* (5304), 1305-1308.
54. Sode, O.; Voth, G. A., Electron transfer activation of a second water channel for proton transport in [FeFe]-hydrogenase. *J Chem Phys* **2014**, *141* (22), 22D527.
55. Kerns, S. J.; Agafonov, R. V.; Cho, Y.-J.; Pontiggia, F.; Otten, R.; Pachov, D. V.; Kutter, S.; Phung, L. A.; Murphy, P. N.; Thai, V.; Alber, T.; Hagan, M. F.; Kern, D., The energy landscape of adenylate kinase during catalysis. *Nat Struct Mol Biol* **2015**, *22* (2), 124-131.
56. Welborn, V. V.; Head-Gordon, T., Computational design of synthetic enzymes. *Chem Rev* **2018**, *119* (11), 6613-6630.
57. Reilley, D. J.; Popov, K. I.; Dokholyan, N. V.; Alexandrova, A. N., Uncovered dynamic coupling resolves the ambiguous mechanism of phenylalanine hydroxylase oxygen binding. *J Phys Chem B* **2019**, *123* (21), 4534-4539.
58. Arrigoni, F.; Bertini, L.; Bruschi, M.; Greco, C.; de Gioia, L.; Zampella, G., H<sub>2</sub> Activation in [FeFe]-hydrogenase cofactor versus diiron dithiolate models: Factors underlying the catalytic success of nature and implications for an improved biomimicry. *Chem: Eur J* **2019**, *25* (5), 1227-1241.
59. Artz, J. H.; Zadvornyy, O. A.; Mulder, D. W.; King, P. W.; Peters, J. W., *Structural characterization of poised states in the oxygen sensitive hydrogenases and nitrogenases*. 1 ed.; Elsevier Inc.: 2017; Vol. 595, p 213-259.

60. Hoffman, B. M.; Lukoyanov, D.; Yang, Z.-Y.; Dean, D. R.; Seefeldt, L. C., Mechanism of nitrogen fixation by nitrogenase: The next stage. *Chem Rev* **2014**, *114* (8), 4041-4062.
61. McKee, M. L., A New Nitrogenase Mechanism Using a CFe<sub>8</sub>S<sub>9</sub> Model: Does H<sub>2</sub> elimination activate the complex to N<sub>2</sub> addition to the central carbon atom? *J Phys Chem A* **2015**, *120* (5), 754-764.
62. Rao, L.; Xu, X.; Adamo, C., Theoretical investigation on the role of the central carbon atom and close protein environment on the nitrogen reduction in Mo nitrogenase. *ACS Catal* **2016**, *6* (3), 1567-1577.
63. Siegbahn, P. E. M., Model calculations suggest that the central carbon in the FeMo-cofactor of nitrogenase becomes protonated in the process of nitrogen fixation. *J Am Chem Soc* **2016**, *138* (33), 10485-10495.
64. Cardenas, A. J. P.; Ginovska, B.; Kumar, N.; Hou, J.; Raugei, S.; Helm, M. L.; Appel, A. M.; Bullock, R. M.; O'Hagan, M., Controlling proton delivery through catalyst structural dynamics. *Angew Chem Int Ed* **2016**, *128* (43), 13707-13711.
65. Hou, J.; Fang, M.; Cardenas, A. J. P.; Shaw, W. J.; Helm, M. L.; Bullock, R. M.; Roberts, J. A. S.; O'Hagan, M., Electrocatalytic H<sub>2</sub> production with a turnover frequency 10<sup>7</sup>s<sup>-1</sup>: the medium provides an increase in rate but not overpotential. *Energy Environ Sci* **2014**, *7* (12), 4013-4017.
66. Curtis, C. J.; Miedaner, A.; Ciancanelli, R.; Ellis, W. W.; Noll, B. C.; Rakowski DuBois, M.; DuBois, D. L., [Ni(Et 2PCH 2NMeCH 2PEt 2) 2]<sup>2+</sup> as a Functional Model for Hydrogenases. *Inorg Chem* **2003**, *42* (1), 216-227.
67. DuBois, D. L.; Bullock, R. M., Molecular electrocatalysts for the oxidation of hydrogen and the production of hydrogen - The role of pendant amines as proton relays. *Eur J Inorg Chem* **2011**, *2011* (7), 1017-1027.
68. Pool, D. H.; Stewart, M. P.; O'Hagan, M.; Shaw, W. J.; Roberts, J. A. S.; Bullock, R. M.; DuBois, D. L., Acidic ionic liquid/water solution as both medium and proton source for electrocatalytic H<sub>2</sub> evolution by [Ni(P<sub>2</sub>N<sub>2</sub>)<sub>2</sub>]<sup>2+</sup> complexes. *Proc Natl Acad Sci USA* **2012**, *109* (39), 15634-15639.
69. Klug, C. M.; Cardenas, A. J. P.; Bullock, R. M.; O'Hagan, M.; Wiedner, E. S., Reversing the tradeoff between rate and overpotential in molecular electrocatalysts for H<sub>2</sub> production. *ACS Catal* **2018**, *8* (4), 3286-3296.
70. Dutta, A.; Ginovska, B.; Raugei, S.; Roberts, J. A. S.; Shaw, W. J., Optimizing conditions for utilization of an H<sub>2</sub> oxidation catalyst with outer coordination sphere functionalities. *Dalton Trans* **2016**, *45* (24), 9786-9793.
71. Dutta, A.; Appel, A. M.; Shaw, W. J., Designing electrochemically reversible H<sub>2</sub> oxidation and production catalysts. *Nat Rev Chem* **2018**, 1-9.
72. Priyadarshani, N.; Dutta, A.; Ginovska, B.; Buchko, G. W.; O'Hagan, M.; Raugei, S.; Shaw, W. J., Achieving reversible H<sub>2</sub>/H<sup>+</sup> interconversion at room temperature with enzyme-inspired molecular complexes: A mechanistic study. *ACS Catal* **2016**, *6* (9), 6037-6049.
73. Boralugodage, N. P.; Arachchige, R. J.; Dutta, A.; Buchko, G. W.; Shaw, W. J., Evaluating the role of acidic, basic, and polar amino acids and dipeptides on a molecular electrocatalyst for H<sub>2</sub> oxidation. *Catal Sci Technol* **2017**, *7*, 1108-1121.



74. Dutta, A.; Lense, S.; Roberts, J. A. S.; Helm, M. L.; Shaw, W. J., The Role of Solvent and the Outer Coordination Sphere on H<sub>2</sub> Oxidation Using [Ni(PCy<sub>2</sub>NPyz<sub>2</sub>)<sub>2</sub>]<sup>2+</sup>. *Eur J Inorg Chem* **2015**, 2015 (31), 5218-5225.
75. Dutta, A.; DuBois, D. L.; Roberts, J. A. S.; Shaw, W. J., Amino acid modified Ni catalyst exhibits reversible H<sub>2</sub> oxidation/production over a broad pH range at elevated temperatures. *Proc Natl Acad Sci USA* **2014**, 111 (46), 16286-16291.
76. Raugei, S.; Chen, S.; Ho, M.-H.; Ginovska-Pangovska, B.; Rousseau, R. J.; Dupuis, M.; DuBois, D. L.; Bullock, R. M., The role of pendant amines in the breaking and forming of molecular hydrogen catalyzed by nickel complexes. *Chem: Eur J* **2012**, 18 (21), 6493-6506.
77. Slater, J. W.; Marguet, S. C.; Monaco, H. A.; Shafaat, H. S., Going beyond structure: Nickel-substituted rubredoxin as a mechanistic model for the [NiFe] hydrogenases. *J Am Chem Soc* **2018**, 140 (32), 10250-10262.
78. Slater, J. W.; Shafaat, H. S., Nickel-substituted rubredoxin as a minimal enzyme model for hydrogenase. *J Phys Chem Lett* **2015**, 6 (18), 3731-3736.
79. Slater, J. W.; Marguet, S. C.; Cirino, S. L.; Maugeri, P. T.; Shafaat, H. S., Experimental and DFT investigations reveal the influence of the outer coordination sphere on the vibrational spectra of nickel-substituted rubredoxin, a model hydrogenase enzyme. *Inorg Chem* **2017**, 56 (7), 3926-3938.
80. Zhang, L.; Andersen, E. M. E.; Khajo, A.; Magliozzo, R. S.; Koder, R. L., Dynamic factors affecting gaseous ligand binding in an artificial oxygen transport protein. *Biochemistry-US* **2013**, 52 (3), 447-455.
81. Cook, S. A.; Borovik, A. S., Molecular designs for controlling the local environments around metal ions. *Acc Chem Res* **2015**, 48 (8), 2407-14.
82. Mann, S. I.; Heinisch, T.; Ward, T. R.; Borovik, A. S., Peroxide activation regulated by hydrogen bonds within artificial Cu proteins. *J Am Chem Soc* **2017**, 139 (48), 17289-17292.
83. Mann, S. I.; Heinisch, T.; Weitz, A. C.; Hendrich, M. P.; Ward, T. R.; Borovik, A. S., Modular artificial cupredoxins. *J Am Chem Soc* **2016**, 138 (29), 9073-9076.
84. Doukov, T. I.; Blasiak, L. C.; Seravalli, J.; Ragsdale, S. W.; Drennan, C. L., Xenon in and at the end of the tunnel of bifunctional carbon monoxide dehydrogenase/acetyl-CoA synthase. *Biochemistry-US* **2008**, 47 (11), 3474-3483.
85. Drennan, C. L.; Heo, J.; Sintchak, M. D.; Schreiter, E.; Ludden, P. W., Life on carbon monoxide: X-ray structure of *Rhodospirillum rubrum* Ni-Fe-S carbon monoxide dehydrogenase. *Proc Natl Acad Sci USA* **2001**, 98 (21), 11973-11978.
86. Dobbek, H.; Svetlitchnyi, V.; Gremer, L.; Huber, R.; Meyer, O., Crystal structure of a carbon monoxide dehydrogenase reveals a [Ni-4Fe-5S] cluster. *Science* **2001**, 293 (5533), 1281-1285.
87. Kim, E. J.; Feng, J.; Bramlett, M. R.; Lindahl, P. A., Evidence for a proton transfer network and a required persulfide-bond-forming cysteine residue in Ni-containing carbon monoxide dehydrogenases. *Biochemistry-US* **2004**, 43 (19), 5728-5734.
88. Khadka, N.; Dean, D. R.; Smith, D.; Hoffman, B. M.; Raugei, S.; Seefeldt, L. C., CO<sub>2</sub> reduction catalyzed by nitrogenase: Pathways to formate, carbon monoxide, and methane. *Inorg Chem* **2016**, 55 (17), 8321-30.

89. Peters, J. W.; Schut, G. J.; Boyd, E. S.; Mulder, D. W.; Shepard, E. M.; Broderick, J. B.; King, P. W.; Adams, M. W. W., [FeFe]- and [NiFe]-hydrogenase diversity, mechanism, and maturation. *BBA - Mol Cell Res* **2015**, *1853* (6), 1350-1369.
90. Eisenhart, R. J.; Clouston, L. J.; Lu, C. C., Configuring bonds between first-row transition metals. *Acc Chem Res* **2015**, *48* (11), 2885-2894.
91. Ye, J.; Cammarota, R. C.; Xie, J.; Vollmer, M. V.; Truhlar, D. G.; Cramer, C. J.; Lu, C. C.; Gagliardi, L., Rationalizing the reactivity of bimetallic molecular catalysts for CO<sub>2</sub> hydrogenation. *ACS Catal* **2018**, *8* (6), 4955-4968.
92. Cammarota, R. C.; Vollmer, M. V.; Xie, J.; Ye, J.; Linehan, J. C.; Burgess, S. A.; Appel, A. M.; Gagliardi, L.; Lu, C. C., A bimetallic nickel-gallium complex catalyzes CO<sub>2</sub> hydrogenation via the intermediacy of an anionic d<sup>10</sup> nickel hydride. *J Am Chem Soc* **2017**, *139* (40), 14244-14250.
93. Connelly Robinson, S. J.; Zall, C. M.; Miller, D. L.; Linehan, J. C.; Appel, A. M., Solvent influence on the thermodynamics for hydride transfer from bis(diphosphine) complexes of nickel. *Dalton Trans* **2016**, *45* (24), 10017-10023.
94. Ceballos, B. M.; Tsay, C.; Yang, J. Y., CO<sub>2</sub> reduction or HCO<sub>2</sub> oxidation? Solvent-dependent thermochemistry of a nickel hydride complex. *Chem Commun* **2017**, *53* (53), 7405-7408.
95. Dutta, A.; Roberts, J. A. S.; Shaw, W. J., Arginine-containing ligands enhance H<sub>2</sub> oxidation catalyst performance. *Angew Chem Int Ed* **2014**, *53* (25), 6487-6491.
96. Silver, S. C.; Niklas, J.; Du, P.; Poluektov, O. G.; Tiede, D. M.; Utschig, L. M., Protein delivery of a Ni catalyst to photosystem I for light-driven hydrogen production. *J Am Chem Soc* **2013**, *135* (36), 13246-13249.
97. Mirts, E. N.; Petrik, I. D.; Hosseinzadeh, P.; Nilges, M. J.; Lu, Y., A designed heme-[4Fe-4S] metalloenzyme catalyzes sulfite reduction like the native enzyme. *Science* **2018**, *361* (6407), 1098-1101.
98. Tian, S.; Liu, J.; Cowley, R. E.; Hosseinzadeh, P.; Marshall, N. M.; Yu, Y.; Robinson, H.; Nilges, M. J.; Blackburn, N. J.; Solomon, E. I.; Lu, Y., Reversible nitrosylation in an engineered azurin. *Nat Chem* **2016**, 1-8.
99. Bhagi-Damodaran, A.; Michael, M. A.; Zhu, Q.; Reed, J.; Sandoval, B. A.; Mirts, E. N.; Chakraborty, S.; Moenne-Loccoz, P.; Zhang, Y.; Lu, Y., Why copper is preferred over iron for oxygen activation and reduction in haem-copper oxidases. *Nat Chem* **2017**, *9* (3), 257-263.
100. Schnell, R.; Sandalova, T.; Hellman, U.; Lindqvist, Y.; Schneider, G., Siroheme- and [Fe<sub>4</sub>-S<sub>4</sub>]-dependent NirA from *Mycobacterium tuberculosis* is a sulfite reductase with a covalent Cys-Tyr bond in the active site. *J Biol Chem* **2005**, *280* (29), 27319-28.
101. Laureanti, J. A.; Buchko, G. W.; Katipamula, S.; Su, Q.; Linehan, J. C.; Zadvornyy, O. A.; Peters, J. W.; O'Hagan, M., Protein scaffold activates catalytic CO<sub>2</sub> hydrogenation by a rhodium bis(diphosphine) complex. *ACS Catal* **2018**, *9* (1), 620-625.
102. Natri, F.; Lista, L.; Ringhieri, P.; Vitale, R.; Faiella, M.; Andreatto, C.; Travascio, P.; Maglio, O.; Lombardi, A.; Pavone, V., A heme-peptide metalloenzyme mimetic with natural peroxidase-like activity. *Chem: Eur J* **2011**, *17*, 4444-4453.
103. Bos, J.; Fusetti, F.; Driessen, A. J. M.; Roelfes, G., Enantioselective artificial metalloenzymes by creation of a novel active site at the protein dimer interface. *Angew Chem Int Ed* **2012**, *51* (30), 7472-7475.

104. Bos, J.; Roelfes, G., Artificial metalloenzymes for enantioselective catalysis. *Curr Opin Chem Biol* **2014**, *19*, 135-143.
105. Drienovská, I.; Ríoz-Martínez, A.; Draksharapu, A.; Roelfes, G., Novel artificial metalloenzymes by in vivo incorporation of metal-binding unnatural amino acids. *Chem Sci* **2014**, *6*, 770-776.
106. Villarino, L.; Splan, K. E.; Reddem, E.; Alonso-Cotchico, L.; Gutiérrez de Souza, C.; Lledós, A.; Maréchal, J.-D.; Thunnissen, A.-M. W. H.; Roelfes, G., An artificial heme enzyme for cyclopropanation reactions. *Angew Chem Int Ed* **2018**, *57* (26), 7785-7789.
107. Yang, H.; Srivastava, P.; Zhang, C.; Lewis, J. C., A general method for artificial metalloenzyme formation through strain-promoted azide-alkyne cycloaddition. *ChemBiochem* **2014**, *15* (2), 223-7.
108. Srivastava, P.; Yang, H.; Ellis-Guardiola, K.; Lewis, J. C., Engineering a dirhodium artificial metalloenzyme for selective olefin cyclopropanation. *Nat Commun* **2015**, *6* (1).
109. Grimm, A. R.; Sauer, D. F.; Davari, M. D.; Zhu, L.; Bocola, M.; Kato, S.; Onoda, A.; Hayashi, T.; Okuda, J.; Schwaneberg, U., Cavity size engineering of a  $\beta$ -barrel protein generates efficient biohybrid catalysts for olefin metathesis. *ACS Catal* **2018**, 3358-3364.
110. Walsh, A. P.; Laureanti, J. A.; Katipamula, S.; Chambers, G. M.; Priyadarshani, N.; Lense, S.; Bays, T.; Linehan, J. C.; Shaw, W., Evaluating the impacts of amino acids in the second and outer coordination spheres of Rh bis(diphosphine) complexes for CO<sub>2</sub> hydrogenation. *Faraday Discuss* **2018**.
111. Sommer, D. J.; Vaughn, M. D.; Ghirlanda, G., Protein secondary-shell interactions enhance the photoinduced hydrogen production of cobalt protoporphyrin IX. *Chem Commun* **2014**, *50* (100), 15852-15855.
112. Galan, B. R.; Reback, M. L.; Jain, A.; Appel, A. M.; Shaw, W. J., Electrocatalytic oxidation of formate with nickel diphosphine dipeptide complexes: effect of ligands modified with amino acids. *Eur J Inorg Chem* **2013**, 5366-5371.
113. Khandelwal, S.; Zamader, A.; Nagayach, V.; Dolui, D.; Mir, A. Q.; ORCID: 0000-0002-9998-6329, A. D., Inclusion of peripheral basic groups activates dormant cobalt-based molecular complexes for catalytic H<sub>2</sub> evolution in water. *ACS Catal* **2019**, *9*, 2334-2344.
114. Roy, S.; Nguyen, T.-A. D.; Gan, L.; Jones, A. K., Biomimetic peptide-based models of [FeFe]-hydrogenases: utilization of phosphine-containing peptides. *Dalton Trans* **2015**, *44* (33), 14865-14876.
115. Jones, A. K.; Lichtenstein, B. R.; Dutta, A.; Gordon, G.; Dutton, P. L., Synthetic hydrogenases: incorporation of an iron carbonyl thiolate into a designed peptide. *J Am Chem Soc* **2007**, *129*, 14844-14845.
116. Bacchi, M.; Veinberg, E.; Field, M. J.; Niklas, J.; Matsui, T.; Tiede, D. M.; Poluektov, O. G.; Ikeda-Saito, M.; Fontecave, M.; Artero, V., Artificial hydrogenases based on cobaloximes and heme oxygenase. *ChemPlusChem* **2016**, *81* (10), 1083-1089.
117. Darmon, J. M.; Kumar, N.; Hulley, E. B.; Weiss, C. J.; Raugei, S.; Bullock, R. M.; Helm, M. L., Increasing the rate of hydrogen oxidation without increasing the overpotential: a bio-inspired iron molecular electrocatalyst with an outer coordination sphere proton relay. *Chem Sci* **2015**, *6* (5), 2737-2745.
118. Matson, B. D.; Carver, C. T.; Von Ruden, A.; Yang, J. Y.; Raugei, S.; Mayer, J. M., Distant protonated pyridine groups in water-soluble iron porphyrin electrocatalysts promote selective oxygen reduction to water. *Chem Commun* **2012**, *48* (90), 11100.

119. Rigsby, M. L.; Wasylenko, D. J.; Pegis, M. L.; Mayer, J. M., Medium effects are as important as catalyst design for selectivity in electrocatalytic oxygen reduction by iron–porphyrin complexes. *J Am Chem Soc* **2015**, *137* (13), 4296-4299.
120. Kilgore, U. J.; Stewart, M. P.; Helm, M. L.; Dougherty, W. G.; Kassel, W. S.; DuBois, M. R.; DuBois, D. L.; Bullock, R. M., Studies of a series of  $[\text{Ni}(\text{PR}_2\text{NPh}_2)_2(\text{CH}_3\text{CN})]^{2+}$  complexes as electrocatalysts for H<sub>2</sub> production: Substituent variation at the phosphorus atom of the P<sub>2</sub>N<sub>2</sub> ligand. *Inorg Chem* **2011**, *50* (21), 10908-10918.
121. Wiese, S.; Kilgore, U. J.; DuBois, D. L.; Bullock, R. M.,  $[\text{Ni}(\text{PMe}_2\text{NPh}_2)_2](\text{BF}_4)_2$  as an electrocatalyst for H<sub>2</sub> production. *ACS Catal* **2012**, *2* (5), 720-727.
122. Reback, M. L.; Ginovska-Pangovska, B.; Ho, M.-H.; Jain, A.; Squier, T. C.; Raugei, S.; Roberts, J. A. S.; Shaw, W. J., The role of a dipeptide outer-coordination sphere on H<sub>2</sub>-production catalysts: Influence on catalytic rates and electron transfer. *Chem: Eur J* **2013**, *19* (6), 1928-1941.
123. Jain, A.; Lense, S.; Linehan, J. C.; Raugei, S.; Cho, H.; DuBois, D. L.; Shaw, W. J., Incorporating peptides in the outer-coordination sphere of bioinspired electrocatalysts for hydrogen production. *Inorg Chem* **2011**, *50*, 4073-4085.
124. Ho, M.-H.; O'Hagan, M.; Dupuis, M.; DuBois, D. L.; Bullock, R. M.; Shaw, W. J.; Raugei, S., Water-assisted proton delivery and removal in bio-inspired hydrogen production catalysts. *Dalton Trans* **2015**, *44* (24), 10969-10979.
125. Lense, S.; Dutta, A.; Roberts, J. A. S.; Shaw, W. J., A proton channel allows a hydrogen oxidation catalyst to operate at a moderate overpotential with water acting as a base. *Chem Commun* **2014**, *50* (7), 792-795.
126. Lense, S.; Ho, M. H.; Chen, S. T.; Jain, A.; Raugei, S.; Linehan, J. C.; Roberts, J. A. S.; Appel, A. M.; Shaw, W., Incorporating amino acid esters into catalysts for hydrogen oxidation: steric and electronic effects and the role of water as a base. *Organometallics* **2012**, *31* (19), 6719-6731.
127. Yang, J. Y.; Smith, S. E.; Liu, T.; Dougherty, W. G.; Hoffert, W. A.; Kassel, W. S.; DuBois, M. R.; DuBois, D. L.; Bullock, R. M., Two pathways for electrocatalytic oxidation of hydrogen by a Nickel bis(diphosphine) complex with pendant amines in the second coordination sphere. *J Am Chem Soc* **2013**, *135* (26), 9700-9712.
128. Dutta, A., Lense, S., Hou, J., Engelhard, M., Roberts, J. A. S., Shaw, W. J., Minimal proton channel enables H<sub>2</sub> oxidation and production with a water soluble nickel-based catalyst. *J Am Chem Soc* **2013**, *135*, 18490-18496.
129. Das, P.; Ho, M.-H.; O'Hagan, M.; Shaw, W. J.; Morris Bullock, R.; Raugei, S.; Helm, M. L., Controlling proton movement: electrocatalytic oxidation of hydrogen by a nickel( ii) complex containing proton relays in the second and outer coordination spheres. *Dalton Trans* **2014**, *43* (7), 2744-2754.
130. Smith, S. E.; Yang, J. Y.; DuBois, D. L.; Bullock, R. M., Reversible electrocatalytic production and oxidation of hydrogen at low overpotentials by a functional hydrogenase mimic. *Angew Chem Int Ed* **2012**, *51* (13), 3152-3155.
131. Stachura, M.; Chakraborty, S.; Gottberg, A.; Ruckthong, L.; Pecoraro, V. L.; Hemmingsen, L., Direct observation of nanosecond water exchange dynamics at a protein metal site. *J Am Chem Soc* **2016**, *139* (1), 79-82.

132. Stachura, M.; Chakraborty, S.; Gottberg, A.; Ruckthong, L.; Pecoraro, V. L.; Hemmingsen, L., Direct observation of nanosecond water exchange dynamics at a protein metal site. *J Am Chem Soc* **2017**, *139* (1), 79-82.
133. Roy, S.; Sharma, B.; Pécaut, J.; Simon, P.; Fontecave, M.; Tran, P. D.; Derat, E.; Artero, V., Molecular cobalt complexes with pendant amines for selective electrocatalytic reduction of carbon dioxide to formic acid. *J Am Chem Soc* **2017**, *139* (10), 3685-3696.